

## Durham E-Theses

---

*Genetic interactions between PXY and the ERECTA and PLETHORA gene families drive cell size and cell proliferation during vascular development in Arabidopsis thaliana.*

CONNOR, KATHERINE,ALEXANDRA

### How to cite:

---

CONNOR, KATHERINE,ALEXANDRA (2020) *Genetic interactions between PXY and the ERECTA and PLETHORA gene families drive cell size and cell proliferation during vascular development in Arabidopsis thaliana.*, Durham theses, Durham University. Available at Durham E-Theses Online:  
<http://etheses.dur.ac.uk/13654/>

### Use policy

---

The full-text may be used and/or reproduced, and given to third parties in any format or medium, without prior permission or charge, for personal research or study, educational, or not-for-profit purposes provided that:

- a full bibliographic reference is made to the original source
- a [link](#) is made to the metadata record in Durham E-Theses
- the full-text is not changed in any way

The full-text must not be sold in any format or medium without the formal permission of the copyright holders.

Please consult the [full Durham E-Theses policy](#) for further details.

---

Academic Support Office, Durham University, University Office, Old Elvet, Durham DH1 3HP  
e-mail: [e-theses.admin@dur.ac.uk](mailto:e-theses.admin@dur.ac.uk) Tel: +44 0191 334 6107  
<http://etheses.dur.ac.uk>

**GENETIC INTERACTIONS BETWEEN PXY AND  
THE ERECTA AND PLETHORA GENE FAMILIES  
DRIVE CELL SIZE AND CELL PROLIFERATION  
DURING VASCULAR DEVELOPMENT IN  
ARABIDOPSIS THALIANA.**

By Katherine Connor

DURHAM UNIVERSITY

Dedicated to Penelope Aoun.

Thank you for being the greatest and most supportive lab partner and true friend.

With special thanks to Dr. Peter Etchells for being the most inspiring and encouraging supervisor, without whom I would not have had the courage to pursue my passion for science. Further, Dr. Tim Hawkins and Christine Richardson of whom their dedication and assistance within the microscopy department is truly valued and appreciated.

# CONTENTS

## Table of Contents

<b>1. GENERAL INTRODUCTION</b>	<b>7</b>
Meristem function and organisation	7
Vascular morphology of shoots and roots	11
Regulators of vascular development	13
Vascular anatomy	19
Aims and Objectives	23
Broader impact of the research	24
<b>2. METHODS</b>	<b>26</b>
3.1 Seed stocks	26
3.2 PCR analysis	26
3.3 Preparation of media for plant growth	27
3.4 Sowing of plant seeds	27
3.5 Harvesting of plant material	27
3.6 Preparation for anatomical sectioning	27
3.7 Embedding of JB4 samples	28
3.8 Sectioning and visualization JB4 embedded samples	28
3.9 Quantification of cell numbers	28
3.10 Radii quantification	28
3.11 ClearSee for GFP reporter visualization	29
3.12 GUS staining and Technovit embedding	29
3.13 Yeast-2-hybrid	29
<b>3. ERECTA STORY; VASCULAR DEVELOPMENT IN THE STEM</b>	<b>33</b>
Background	33
Aims and objectives	34
Results	34
Phenotypic results of <i>pxf erf</i> sextuple mutants	34
Quantitative morphology of PXf and ERf mutant combinations	35
Discussion	39
<b>4. SEEDLING STORY; THE INITIATION OF SECONDARY GROWTH</b>	<b>40</b>
Background	40
Aims and objectives	43
The Plethora story	46
Aims and objectives	47
Results	48



Genetic interactions between <i>PXY</i> signalling and <i>PLT</i> genes .....	53
Discussion .....	56
<b>5. GENERATING TOOLS TO FURTHER UNDERSTAND AUXIN AND PIN LOCALISATION BEHAVIOUR REGARDING SECONDARY GROWTH INITIATION.</b> .....	57
Background .....	57
Imaging and visualization of vascular morphology through microscopy .....	61
Aims and objectives.....	63
Results.....	64
Discussion .....	66
<b>6. INVESTIGATING INTERACTIONS BETWEEN TMO6 &amp; WOX14 TRANSCRIPTION FACTORS</b> .....	67
Background .....	67
Aims and objectives.....	72
Results.....	72
Discussion .....	73
<b>7. GENERAL DISCUSSION</b> .....	74
Implications of this research .....	75
<b>8. REFERENCES</b> .....	77

## LIST OF FIGURES

**Figure 1:** Apical meristem of a growing root tip showing: (1) central zone, (2) peripheral zone, (3) medullary (i.e. central) meristem, (4) medullary tissue..... 8

**Figure 2:** Root apical meristematic structure; Pericycle, responsible for the formation of lateral roots by rapidly dividing near the xylem elements of the root, companion cell, closely associated to sieve elements; protophloem sieve elements, the main organizers of the phloem pole; metaphloem sieve elements, developed after those of the protophloem; phloem initial, responsible for movement of macromolecules and proteins such as sugars and mRNAs; intervening procambial cells, meristematic tissue; protoxylem, spiral thickening of which provides the mechanical strength to the cell; metaxylem, formed after previous protoxylem; outer cell layers; quiescent centre, region in which cell division is very slow and a proposed initiator of signalling; vascular initials..... 10

Figure 3: Diagram to show conductive transport of water, macromolecules and proteins throughout the plant as transported by the xylem and phloem conductive tissues..... 12

Figure 4: Model diagram of the genetic interaction between the CLE41 gene and its encoded protein TDIF (ligand) with the complementary PXY receptor. .... 15

**Figure 5:** Comparative histological sections of *Arabidopsis thaliana* across multiple genetic backgrounds. Horizontal cross sections of Toluidine-blue stained hypocotyls showing the vascular bundles (D-H). The pxy mutant (E) shows a reduced vascular bundle in comparison to WT/Col (D). The 35S::CLE41 mutant shows increased vascular bundle size in (F). Sections stained with Aniline blue are shown (I-M) with phloem fluorescing green on the outside. This is greatly disrupted in mutants K and L. Transverse toluidine-blue sections are

shown (N-R). Mutations in pxy shown in (O) comparative to WT/Col in (N) identify loss in organisational plane. (Etchells & Turner, 2010). ..... 17

**Figure 6:** Cross section of the root tip showing the specific cell types and layers colour coded appropriately. Highlights the Quiescent centre and vascular bundle initials during primary growth. (Figure taken from: <https://www.psb.ugent.be/root-development/302-introduction>) 21

**Figure 7:** Stem tissue from *pxf erf* lines showing the vascular bundles across genetic lines and the identification of cell types utilised for calculating cell size. (A) Wild-type, (B) *erf*, (C) *pxf*, (D) *pxf erf erl2*, (E) *pxf erf* vascular bundles. Phloem arrangement is marked with red arrows. Cells with phloem cap-like morphology are marked with asterisks. Scale bars: 50  $\mu\text{m}$ ; xv, xylem vessel; pc, procambium; ph, phloem; ph-c, phloem cap; en, endodermis. .... 37

**Figure 8:** Comparisons of morphology of cells in stem vascular bundles. (A-C) Boxplots on left show mean cell perimeter for xylem vessels (A), xylem fibres (B) and phloem cells (C). Boxes represent the 25th to 75th percentile, the horizontal line marks the median. Whiskers' endpoints are the min/max points within the interval spanning  $Q1-1.5*IQR$  (lower) and  $Q3-1.5*IQR$  (upper). Asterisks mark significant differences (ANOVA plus Tukey; \*\*\* $P<0.001$ , \*\* $P<0.01$ ; ] Ridgeline plots on the right show the distributions of cell areas divided into quartiles. Areas of *pxf erf* lines were greater than those of *pxf erf erl2* lines in all three cell types ( $P\leq 0.05$ ). Differences were calculated with ANOVA and a Tukey post-hoc test. .... 38

**Figure 9:** GO Analysis data utilised for identification of target genes. (A) shows a 7 day old Arabidopsis seedling and the locations of cut sections on the hypocotyl and root. (B-D) Show horizontal cross sections of the respective sections (upper row from the hypocotyl and lower row from the root). The xylem pole axis is indicated with the asterisks and the phloem poles indicated by the red arrows. This shows the increase in cellular proliferation as observed in the overexpression 35S::CLE41 background, and lack of cellular proliferation in pxy. (E & H) Show gene ontology analysis of two of the comparisons from the RNA-seq data. This identifies key gene categories. (F) Shows a Venn diagram used to identify genes that were mis-expressed in multiple data sets. PLT genes are marked (with a couple of others as identified for further explorative study within this thesis.). (G) Shows the normalised gene counts for PLT genes from the RNA-seq data. .... 45

**Figure 10:** Transverse cross sections taken at 7 days of growth of the Arabidopsis seedling root. Sections are stained with Toluidine-blue. The primary xylem initials are marked by red asterisks. Little qualitative morphological differences of significance observed between genotypes. .... 50

**Figure 11:** Transverse cross sections taken at 14 days of growth of the Arabidopsis seedlings. Sections are stained with Toluidine-blue. The primary xylem initials are marked by red asterisks. Little qualitative morphological differences of significance observed between genotypes. .... 51

**Figure 12:** Transverse cross sections taken at 28 days of growth of the Arabidopsis seedlings. Sections are stained with Toluidine-blue. There are obvious morphological differences between genotypes at this stage, when secondary growth is well established. There is distinct loss of organisation within the 35S::CLE41 overexpression backgrounds. In pxy mutation backgrounds there also is an overall size reduction of root radii. The pxy *plt3 plt5* shows a clear enhancement of the pxy phenotype in (F). There is a suppression of cell proliferation in the 35S::CLE41 background shown in (D) comparative to (C) and (A). Xylem cells or cell bundles are marked by red asterisk. .... 52

**Figure 13:** Cell radii across genotypes for quantification purposes. (A-F) Show example images utilised for cell radii calculations and a comparison between the genotypes. Shown here is the observable difference between pxy *plt5* double mutant and pxy *plt3 plt5* triple mutant. (G & F) Show graphically the comparison between genotypes for the radii (G) and xylem vessel number (H). This identifies the observational difference between *plt5* mutation

in the respective pxy and 35S::CLE41 compared to plt3 and plt5 in the same backgrounds. This highlights the redundancy and reliance on both genes of PLT3 and PLT5.....	55
<b>Figure 14:</b> Auxin homeostasis is essential for proper development. Drawings of a wild-type seedling and an adult plant (centre of the figure in green) and some characterized mutants for auxin homeostasis (in boxes). Mutants with affected auxin biosynthesis are in light brown boxes. sur1 is an overproducer [5] while wei8 tar2 [6] is depleted of auxin. Signalling mutants are shown in light blue boxes and are mutated in the auxin transcription factor 5 (arf5/monopteros) [25], auxin transcriptional inhibitor iaa14 (or solitary root) [26], or the auxin co-receptors (tir1, afb2, afb3) [27]. Mutants for influx (aux1) [28] and efflux auxin transporters (pin1) [7] are shown in the light red boxes (Paque & Weijers., 2016).....	59
<b>Figure 15:</b> Showing the Aux/IAA interaction at both high and low auxin levels. (A) Ontogeny of the xylem tissues during embryogenesis. Two provascular initial cells share a cellular connection and receive more auxin than the other two through the incipient cotyledons forming above (indicated as asterisk next to early xylem in the e xylem in the early globular stage embryo). These cells will form the xylem axis of the root and are marked by high auxin signalling. The other provascular cells will form procambium and phloem cell lineages, with the procambium marked by high cytokinin (CK) signalling. (B) Schematic longitudinal (lower panel) and radial (upper panel) cross-section through the vascular bundle of the root apical meristem. (C) The Auxin- TMO5/LHW-LOG4-CK pathway controls growth and patterning of the vascular bundle through local production of CK along the xylem axis, which triggers periclinal cell divisions (PD) in the neighbouring procambium cells. (D) Summary of regulatory connections included in computational models describing vascular patterning in the root meristem. (E) The AHL proteins are expressed in procambium cells and migrate towards the xylem axis, thereby controlling strict boundaries between xylem and procambium through an unknown mechanism. (F) Control of metaxylem versus protoxylem identity by the SHR-miR165/166-HD-ZIPIII pathway. (De Rybel, Mähönen, Helariutta & Weijers., 2015).....	60
<b>Figure 16:</b> “Consequences of Removing the Feed-Forward Loop.(A) to (E) Morphology of vascular bundles from inflorescence stems in the wild type (A), lbd4 wox14 (B), lbd4 tmo6 (C), tmo6 wox14 (D), and wox14 lbd4 tmo6 (E). Transverse sections were stained with toluidine blue. Insets show closeups of the cambium (green). pc, cambium; ph, phloem; x, xylem. Brackets mark the vascular bundle size along the radial axis of the stem. Bars = 50 µm.(F) Boxplots showing mean number of cells per vascular bundle in wox14 lbd4 tmo6 and double and single mutant controls. Significant differences were determined by ANOVA with an LSD posthoc test (n = 6). (G) Boxplot showing vascular bundle shape determined by measuring the ratio of tangential to radial axis (n = 6). Boxplots show median (inner line) and inner quartiles (box). Whiskers extend to the highest and lowest values no greater than 1.5 times the inner quartile range, and circles show outliers.” (Smit et al., 2020).....	70
<b>Figure 17:</b> Graphical results: Nicotiana leaf protoplasts were transformed with a construct that harboured LBD4pro::LUC (LUCIFERASE). LUC activity in cells co-transformed with both LBD4pro::LUC reporter and a 35S::TMO6 construct, was higher than that observed in cells transformed with the LBD4pro::LUC reporter with a control. LBD4 promoter activity was further increased when cells were co-transformed with both LBD4pro::LUC, 35S::TMO6, and 35S::WOX14 plasmids (Provided in full by Heng, Unpublished) .....	71
<b>Figure 18:</b> Theoretical diagram for yeast two hybrid system testing set up. Wox14 and TMO6 ORF sizes are 65 and 55 respectively.....	73

## LIST OF TABLES

<b>Table 1:</b> Primers utilised for genotyping of seed lines. Primers obtained from previously publications.....	26
<b>Table 2:</b> Primer designed for WOX14. [] brackets indicate inclusion of restriction enzyme sites.....	31
<b>Table 3:</b> Primers designed for TMO6. [] brackets indicate inclusion of restriction enzyme sites.....	32

# 1. GENERAL INTRODUCTION

## **Meristem function and organisation**

In animals, development occurs in such a way that it is directed towards a pre-determined body plan. Plants, on the other hand, show iterative growth where architecture is a consequence of growth and adaption in response to environmental cues. It is this ability of plant systems that makes their development an intriguing area of research. In higher plant systems, post-embryonic tissues are derived from pluripotent cells found in niches termed the meristems. Meristematic cells are undifferentiated and pluripotent. Their fate is not pre-determined and as such they can generate all the cell types within the plant. Meristematic tissue is characterised by small cells with thin cell walls, large nuclei, absent or small vacuoles and little intracellular space. The structural cell wall of mature plant cells does not allow migration of cells throughout the system, the result of which being that plant development is rooted in differential growth from these meristematic cells held in niches. Because meristems are the driving force behind growth within higher plant systems, they also underpin their unique ability to develop in response to external stimuli due to their sessile life style.

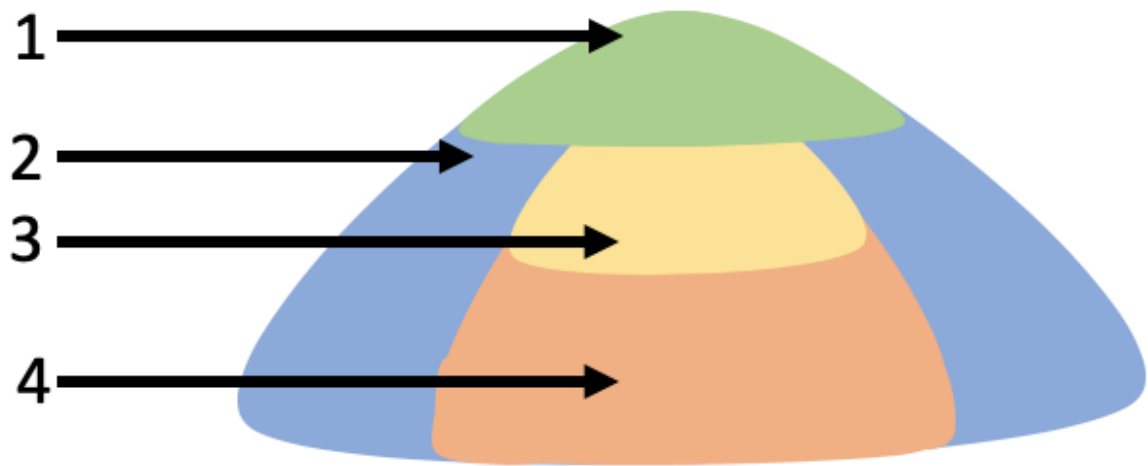


**Figure 1:** Apical meristem of a growing root tip showing: (1) central zone, (2) peripheral zone, (3) medullary (i.e. central) meristem, (4) medullary tissue.

Apical meristems are responsible for length-wise growth and contain organogenic cells that are established during embryogenesis (Hay & Tsiantis, 2006). They reside in the growing root and shoot tips of the plant; termed the root apical meristem (RAM) and the shoot apical meristem (SAM). The SAM and RAM divide rapidly and are considered indeterminate as they do not possess a defined end fate. Typically, the SAM gives rise to above ground plant organs such as the leaves and flowers. The RAM is responsible for divisions that result in the formation and growth of roots. It harbours an organising centre, termed the quiescent centre (Figure 2, 6) that orchestrates the division and organisation of cells within two dimensions.

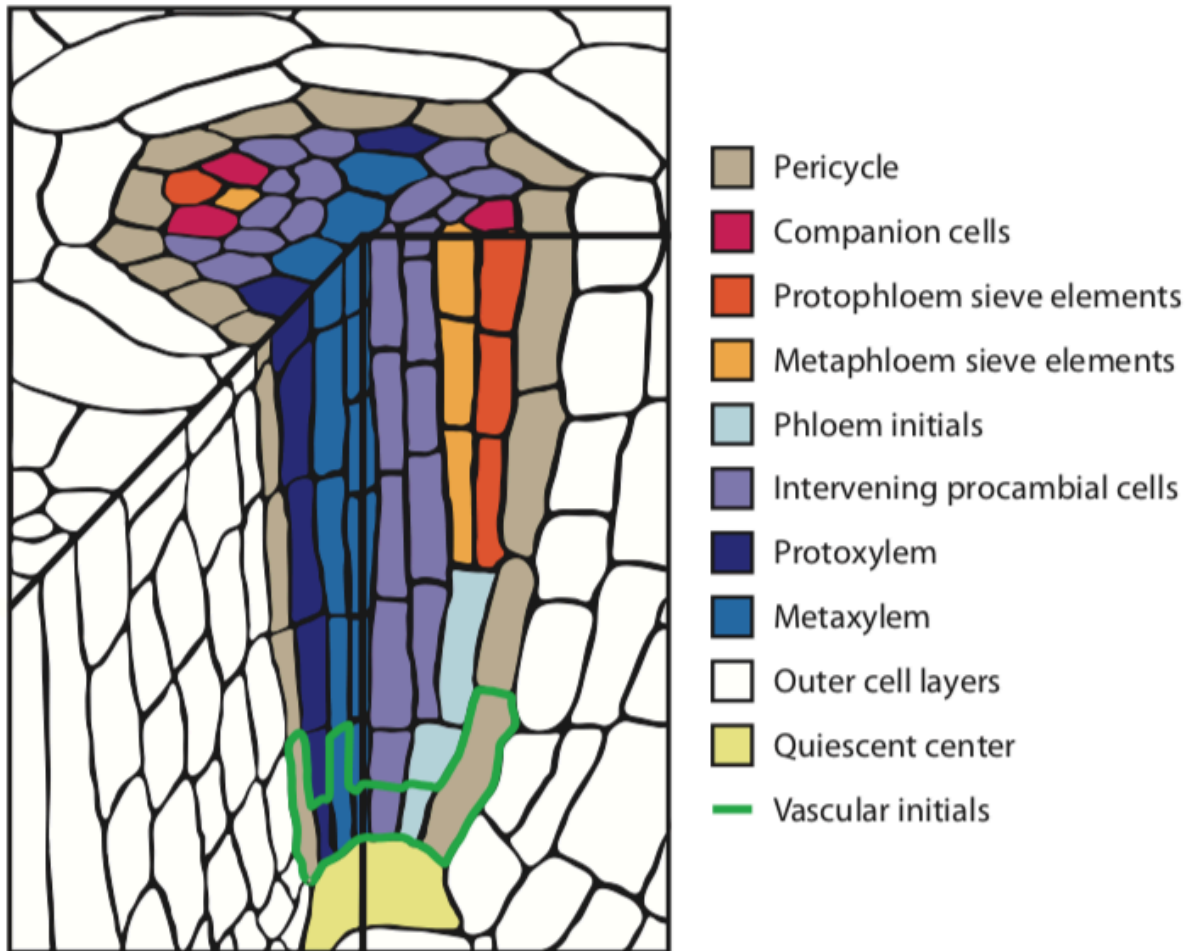


**Figure 2:** Root apical meristematic structure; Pericycle, responsible for the formation of lateral roots by rapidly dividing near the xylem elements of the root, companion cell, closely associated to sieve elements; protophloem sieve elements, the main organizers of the phloem pole; metaphloem sieve elements, developed after those of the protophloem; phloem initial, responsible for movement of macromolecules and proteins such as sugars and mRNAs; intervening procambial cells, meristematic tissue; protoxylem, spiral thickening of which provides the mechanical strength to the cell; metaxylem, formed after previous protoxylem; outer cell layers; quiescent centre, region in which cell division is very slow and a proposed initiator of signalling; vascular initials.



The meristematic niches of plant systems are found not only in the apical RAM and SAM, but also at the buds and nodes of the stem. These are defined as the intercalary meristematic tissue and located at nodes of monocots, such as bamboo, responsible for driving stem elongation. Finally, the vascular meristems, the cambium and procambium are present between the xylem and phloem, and also constitute a stem cell niche. Sometimes referred to as lateral meristems, they give rise to increases in stem thickness. Genetic and molecular control of the cells in the vascular meristems will be the focus of this thesis.

### **Vascular morphology of shoots and roots**

The movement of resources through the plant body is essential for plant survival as water is taken up from the soil but sugars are assimilated in leaves (Smit & McGregor et al, 2019). The xylem and phloem are the two conductive tissue types of the vascular system and are responsible for the long-distance transport of water and nutrients (Hirakawa, 2010). The xylem tissue transports water and nutrients from the root system to the upper regions of the plant, while phloem distributes photosynthates (Figure 3). Vascular tissue formation is also essential for plant growth as it provides mechanical support for length-wise growth. Vascular development follows a well-structured and complex developmental pattern (Baucher, 2007). The procambium is the lateral meristem that generates the primary tissues of the vascular system. Often arranged in bundles, a single vascular bundle will always contain both xylem and phloem. The cambium which drives secondary (radial) growth and is a continuous cylinder of meristem responsible for the expansion of vascular tissues in mature stems and roots. Thus, cell divisions in the meristematic (pro)cambium, which is located between the xylem (on the inside) and phloem (towards the outside) provides the cells required for their growth. (Mahonen, 2006).

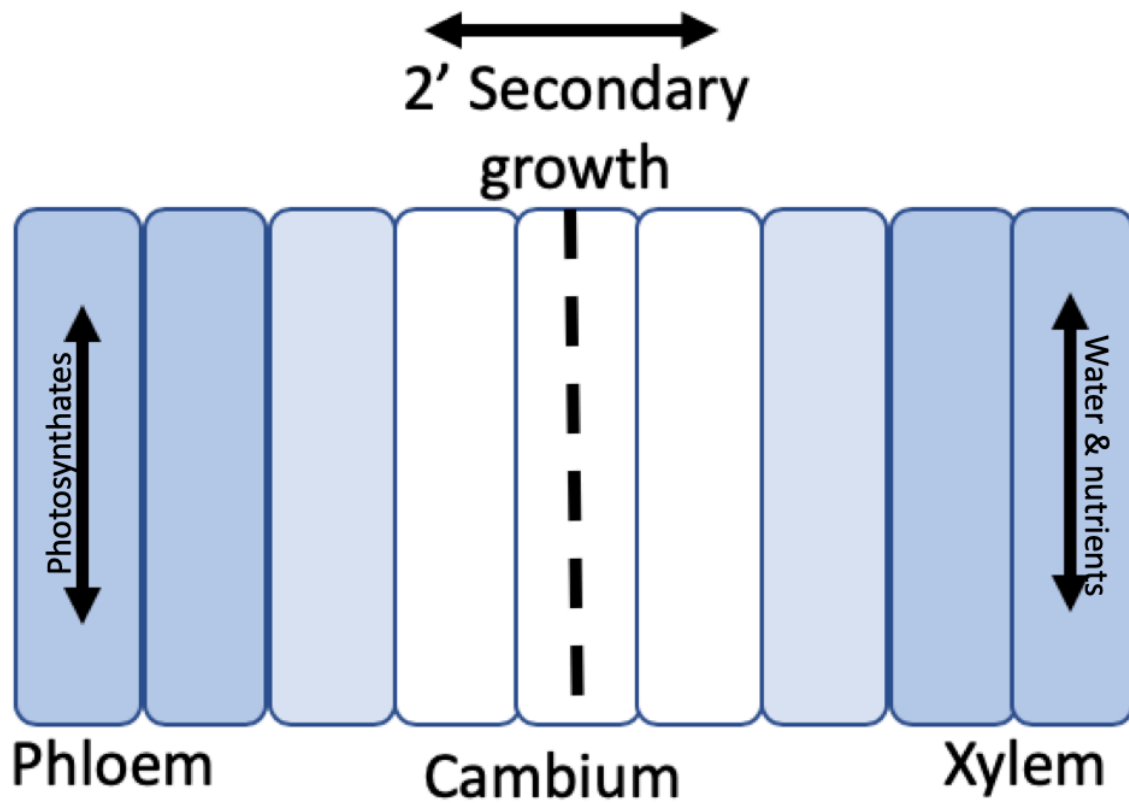


Figure 3: Diagram to show conductive transport of water, macromolecules and proteins throughout the plant as transported by the xylem and phloem conductive tissues.

Xylem cells retain thick secondary cell walls that are rich with lignin, cellulose and hemicellulose (Fàbregas et al, 2015). The xylem tissue comprises vessel elements and tracheids; both are tubular and elongated. At functional maturity tracheids and vessel elements have undergone programmed cell death, facilitating water movement in part due to their arrangement with perforations, termed pits, adjacent between cells, eliminating a barrier for transport. Their secondary cell walls are hardened with lignin in order to provide structural support. Phloem tissue, on the other hand, is comprised of sieve and companion cells. Sieve cells are arranged in an end-to-end formation with pores, termed sieve plates, between; they are responsible for the conduction of sugar and organic compounds. It is the role of companion cells to support the sieve cells through metabolic support and regulation due to adjacent proximity. Unlike the elements of the xylem, sieve and companion cells are alive at functional maturity; however, they lack cellular structures such as the nucleus and ribosomes. The phloem mediates the transport of autotrophic energy, photoassimilates and signalling molecules such as hormones and peptides (Fàbregas et al, 2015).

### **Regulators of vascular development**

Many genes important for specific developmental processes have been identified by mutation (Embryogenesis in *Drosophila*: Ingham, 1988; Posterior pattern formation in *Drosophila* embryos: Nüsslein-Volhard, 1991; Vulva development in *Caenorhabditis elegans*: Horvitz and Sternberg, 1991; Pattern formation in the *Arabidopsis* embryo: Mayer et al., 1991). Among these, genetic and molecular components have been identified and characterised that are required in *Arabidopsis* to initiate, pattern and expand the vascular tissue. These include a number of phytohormones, components of signalling mechanisms and several transcription factors. One such signalling pathway is characterised by the PHLOEM INTERCALATED WITH XYLEM (PXY) signalling module and is covered in a multitude of existing literature. The PXY gene, sometimes referred to in the literature as TDR (TDIF RECEPTOR) encodes

for a receptor like kinase. PXY was identified in a forward genetic mutagenesis study (Fisher and Turner, 2007). Here, *pxy* mutants were identified as having phloem cells intercalated with xylem cell types, critically lacking the wild type spatial separation (Figure 5). Orientation of growth in wild type plants is perpendicular to the radial axis of the stem in initiating vascular tissue, but alterations to this observed growth orientation were identified in *pxy* mutants (Etchells., 2015). Characteristically, wild type xylem cells are long, straight and run parallel to the apical-basal axis of the stem, but *pxy* mutants were observed with curved xylem cells that run in and out the plane in longitudinal sections (Etchells & Turner, 2010; Figure 5). Thus, PXY was described as controlling vascular organisation. The PXY receptor is localised to the plasma membrane of procambium cells.

The peptide TRACHEARY ELEMENT DIFFERENTIATION INHIBITORY FACTOR (TDIF) encodes PXY's cognate ligand. TDIF is secreted from the phloem. It was first identified as a dodecapeptide that promoted cell division and prevented assumption of tracheary element identity (Ito et al., 2006). The mature TDIF peptide is encoded for by three genes within the CLAVATA3/EMBRYO SURROUNDING REGION (CLE) family; CLE41, CLE42 and CLE44. Photoaffinity labelling demonstrated the binding of TDIF to the PXY receptor (Hirakawa et al, 2008). Cell number increases in the vascular tissue were observed to occur as a result of overexpression of CLE41 (Figure 5), CLE42 and CLE44. These phenotypes are accompanied by gene expression increases in genes that mark dividing cells (Hirakawa et al, 2008; Whitford et al, 2008; Etchells & Turner, 2010). These overexpression phenotypes were found to be entirely suppressed by accompanying *pxy* mutations (Etchells & Turner, 2010). These findings suggest that all known outputs of TDIF signalling are via the PXY receptor (Figure 4) (Etchells & Turner, 2010).

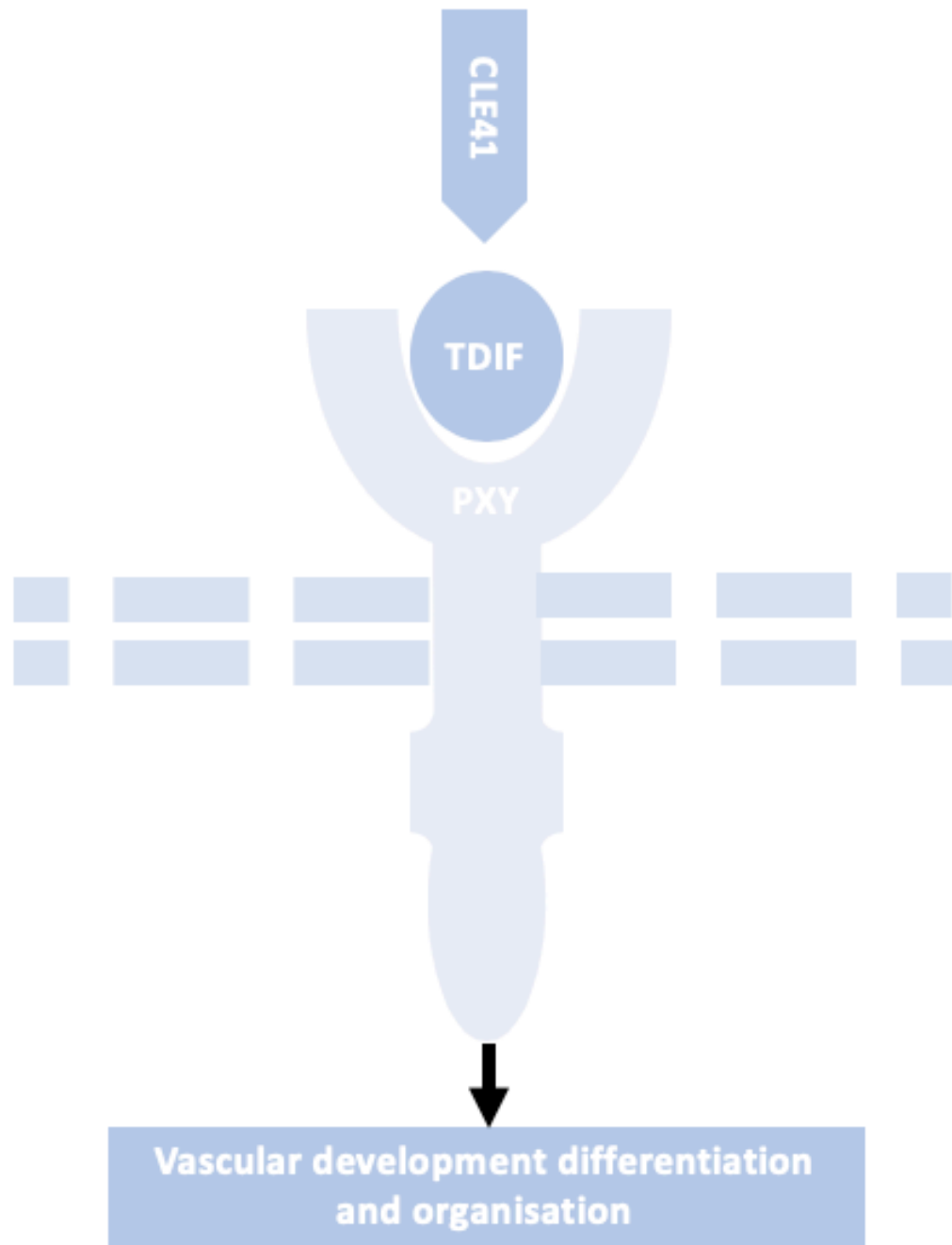
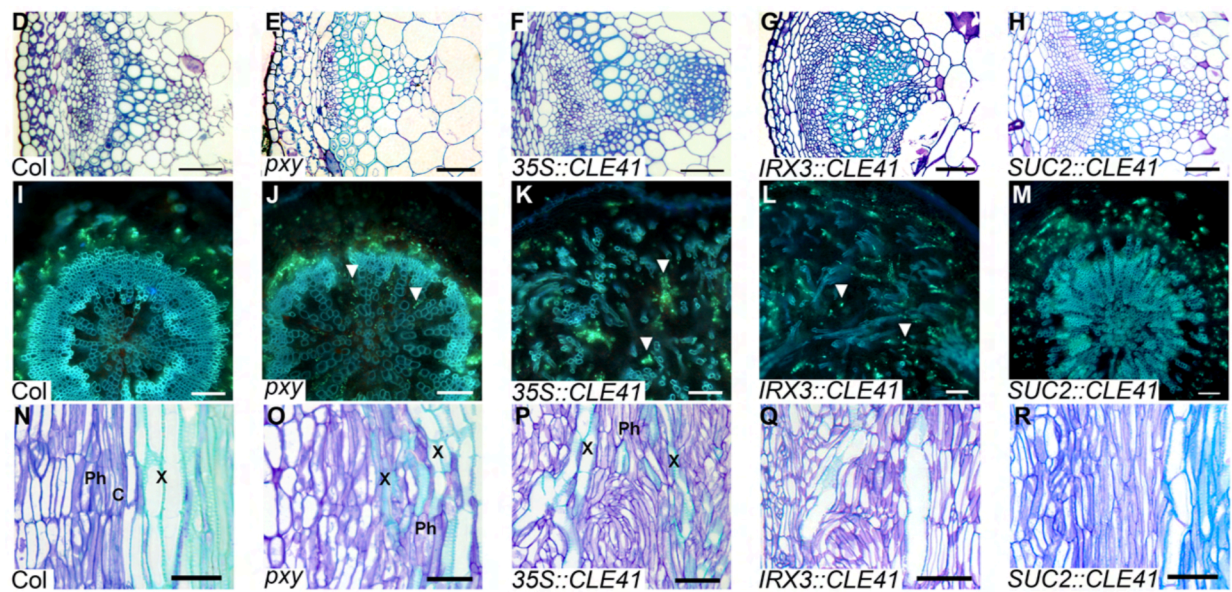


Figure 4: Model diagram of the genetic interaction between the CLE41 gene and its encoded protein TDIF (ligand) with the complementary PXY receptor.

This ligand and receptor pair, TDIF and PXY respectively, have been identified as key regulators of a complex output system. the studies described above demonstrate that they impact the rate of cell division in the procambium and cambium, exclude xylem identity from the division zone and control vascular organisation (Ito et al, 2006; Fisher & Turner, 2007, Hirakawa et al, 2008; Etchells & Turner, 2010).



**Figure 5:** Comparative histological sections of *Arabidopsis thaliana* across multiple genetic backgrounds. Horizontal cross sections of Toluidine-blue stained hypocotyls showing the vascular bundles (D-H). The *pxy* mutant (E) shows a reduced vascular bundle in comparison to WT/Col (D). The *35S::CLE41* mutant shows increased vascular bundle size in (F). Sections stained with Aniline blue are shown (I-M) with phloem fluorescing green on the outside. This is greatly disrupted in mutants K and L. Transverse toluidine-blue sections are shown (N-R). Mutations in *pxy* shown in (O) comparative to WT/Col in (N) identify loss in organisational plane. (Etchells & Turner, 2010).

Mutations in the *PXY* gene result in reductions in the number of vessel cell number, with the ratio of xylem vessels to other cell types reduced (Fisher & Turner, 2007). The observation that *PXY* influences cell-type specification in the xylem adds to what is known about the multifunctional nature of the *PXY* signalling module (Etchells., 2015). *PXY* has been further linked with a second ligand receptor pair characterised by the *ERECTA* (*ER*) receptor, which is phloem expressed (Uchida & Tasake, 2013a) and its cognate ligands *CHALLAL-LIKE2/EPIDERMAL PATTERNING FACTOR-LIKE4* (*CLL2/EPFL4*) and *CHALLAH* (*CHAL/EPFL6*) which are expressed in the endodermis (Abrash et al., 2011; Uchida et al., 2012). *pxy er* double mutants show defects in the organisation of the vasculature greater than that observed in single *pxy* or *er* mutants (Etchells et al., 2013). Within the *Arabidopsis* genome paralogues of *ERECTA* exist. These are *ER-LIKE1* (*ERL1*) and *ER-LIKE2* (*ERL2*) (Shpak et al., 2004). The *ERECTA* family (*ERf*) genes have various roles in the regulation of plant growth and development. They act redundantly promoting cell elongation, cell division, inflorescence architecture (Shpak et al., 2004; Torii et al., 1996), and shoot apical meristem fate (Kimura et al., 2018; Uchida et al., 2013) amongst other roles. In the context of vascular development, *ERf* regulates vascular expansion in the stem (Uchida et al., 2013b) and hypocotyl. It also regulates the timing of xylem fibre formation (Ikematsue et al., 2017; Ragni et al., 2011). Fibre cell types with secondary walls are prevalent in well-established tissues, with parenchymatous cell types dominating in tissue that is younger and less-well established. This change in cell structure, in part, defines the transition to secondary growth. A hallmark loss of *ERf* genes is an increase in cell size, with particular respect to the radial axis (Shpak et al., 2004; Shpak et al., 2003). The interaction between *er* and *pxy* is thought to control vascular organisation but not proliferation. This indicates genetically separable outputs between cell division and vascular organisation (Etchells et al., 2013). The consequence of the interaction between *pxy* and *er* on cell size is yet to be determined.



## Vascular anatomy

The genetic and molecular control of the developmental process through initiation and control of cellular differentiation and proliferation of the vasculature of the root forms the focus of this thesis. The model plant species *Arabidopsis thaliana* is a powerful tool for studying developmental genetics (Meyerowitz, 1989), due to its short generation time and well-annotated genome sequence and consequently it will be the species used in this study. The *Arabidopsis* root is an ideal model for the study of developmental processes that underlie plant vascular development (Wachsman, Sparks and Benfey, 2015). A lack of cell movement within the root structure (as with all plant tissues), and a relative ease of accessibility to microscopic visualisation makes it a powerful developmental model.

*Arabidopsis* primary root anatomy is established during embryogenesis (Dolan et al, 1993). Polarity is established through the primary division of the zygote, forming the apical cell and basal cell. The subsequent division of four provascular initials during this stage establishes the provascular tissue (Scheres et al, 1994). The vascular tissue in the root is initiated at the root tip. Here the morphology is characterised by two developmental axes, the longitudinal, and the radial (Wachsman, Sparks and Benfey, 2015). Longitudinally, cells progress through the differentiation process to a specific fate from stem-cell state in the meristem in three distinct but overlapping zones; meristematic, elongation, and differentiation zone. Radially, the roots of vascular plants are composed of a concentric pattern of cell layers of functionally distinct tissues (Dolan et al, 1993). The characteristic organisation of the root anatomy is comprised of a central cylinder of vascular cells in a so-called diarch formation (Figure 6). Differentiated primary vascular tissue consists of meta- and proto- xylem and phloem, with procambium tissue intervening. Xylem cell lineages are derived from the vascular initials and specified early. The phloem and procambium cell lineages are a direct result of asymmetric periclinal divisions specified within the meristem (Mahonen et al, 2000). Differentiated protophloem

elements are at 90 degrees to two protoxylem elements, the phloem and xylem poles respectively.

Encompassing the vascular cylinder exists the pericycle, endodermis, cortex and finally the epidermis. The main function of the pericycle is providing support, structure and protection for the plant. It is a heterogeneous, non-vascular tissue in plants that is divided into two populations at both the xylem and phloem poles (Beeckman & Smet, 2014). The pericycle has also been linked to xylem loading within the root and within angiosperm roots it is essential for lateral root initiation (Beeckman & Smet, 2014). It is the endodermis layer within the root structure that is responsible for the regulation of water uptake and movement. The endodermis acts as a cylindrical boundary that separates the vascular tissue and functions as an apoplastic barrier for selective nutrient uptake (Miyashima et al., 2011). The cortex layer is comprised mostly of large thin-walled parenchyma cells of the ground tissue system and is surrounded by the single cell layer of the epidermis that provides the final layer to the external environment to protect the plant.

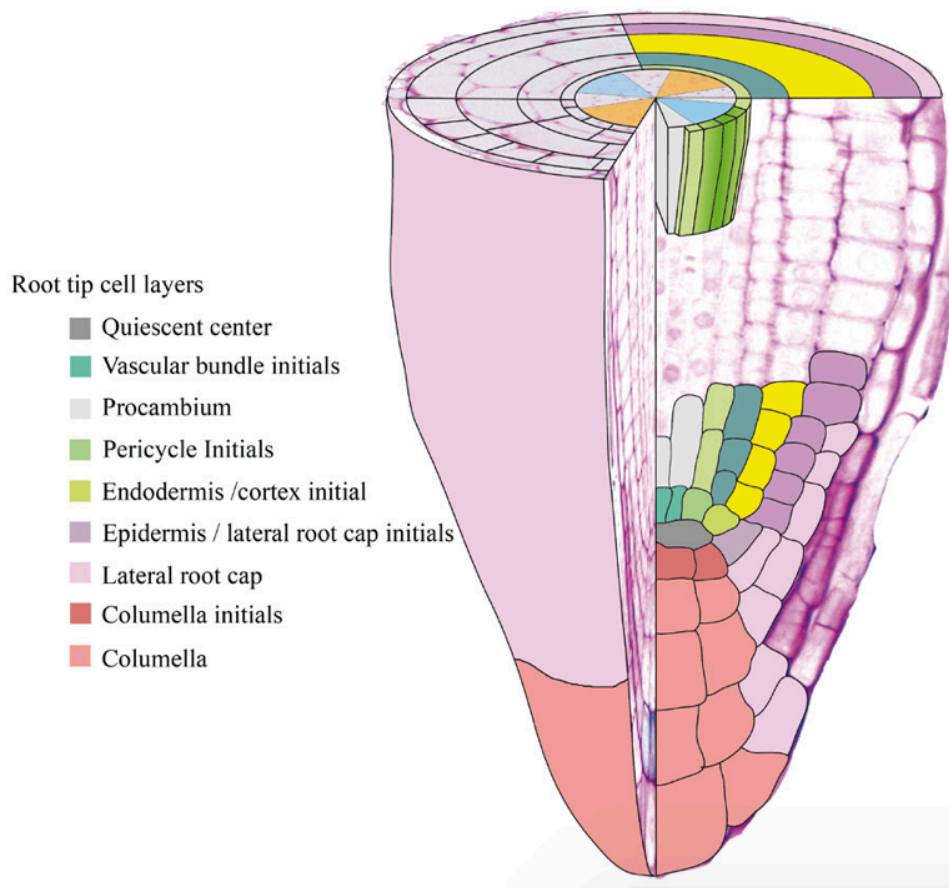
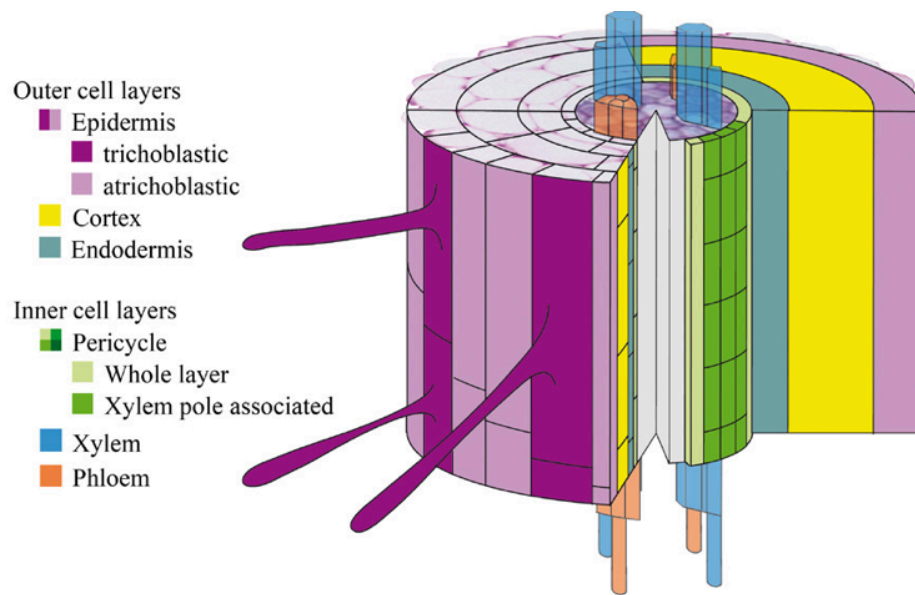


**Figure 6:** Cross section of the root tip showing the specific cell types and layers colour coded appropriately. Highlights the Quiescent centre and vascular bundle initials during primary growth. (Figure taken from: <https://www.psb.ugent.be/root-development/302-introduction>)

Later in development after the initiation of secondary growth has occurred, the diarch pattern described above is lost. The root morphology changes from diarch to, such that cross-section of a dicot root appears to show the xylem tissue in a 'star-like' formation, with cambium present in a ring outside the xylem, and phloem located outside of the cambium. This so-called secondary growth is initiated with divisions in the procambium cells that are the most proximal to the primary xylem established (Baum et al, 2002). Periclinal cell divisions are initiated in the root procambium at approximately five days after germination. Divisions within the pericycle result in the continuous cambial ring formation (Busse and Everett, 1999b). The action of the actively dividing cambium results in secondary xylem and secondary phloem inwards and outwards respectively. For both the root and the hypocotyl of the plant, secondary growth, the lateral growth, of *Arabidopsis* can be defined as two distinct phases. Within the hypocotyl this can be distinguished through the ratio of production of secondary xylem and secondary phloem, with a 'xylem explosion' observed during the secondary phase (Sibout et al, 2008; Ragni et al., 2011). Within both the hypocotyl and root stele, a noticeable distinction between phases is observed through the additional production through division and differentiation of xylem fibres and xylem vessels (Fàbregas et al, 2015).

The embryo of *Arabidopsis* does not contain functional xylem or phloem cells (Busse and Evert, 1999); however, prior to germination, several of the known genes of vascular differentiation are already expressed. Embryogenesis is known to be hormonally regulated, with auxin playing a major role (Friml et al, 2003). The primary cell types of *Arabidopsis* are produced from the initials that surround the quiescent centre predefined during embryogenesis (Van den Berg et al, 1997). Here the diarch pattern of the primary phloem and procambial cells flanking the central xylem axis is established. The secondary growth stage is characterised as the radial expansion. Proliferation of cells in the cambium results in the formation of secondary

xylem (tracheids and vessel elements) and phloem (sieve elements and companion cells). Auxin regulates this transition in conjunction with the PXY receptor. Secondary growth is mediated by the vascular cambium the cell-proliferation activity of which is regulated by long distance by auxin transport (Agusti et al., 2011). Many of the genes that are upregulated within wood-forming stems have auxin responsive cis-acting elements within their promoter region, supporting the idea that auxin is central to the regulation of this system (Jae-Heung Ko, Park & Yang, 2004). Smetana et al (2019) found that high levels of auxin signalling define an organiser in the cambium, and that locally high levels of auxin within the root vasculature are sufficient to establish this organiser cell which promotes stem-cell-like divisions and identity in adjacent cells (Smetana et al., 2019). This local maximum of auxin, occurs as a consequence expression of CLASS III HOMEODOMAIN-LEUCINE ZIPPER (HD-ZIP III) transcription factors, which promotes xylem identity and cellular quiescence of the organiser cells during primary development (Smetana et al., 2019). Auxin response markers have shown local maxima within the xylem domain of the vasculature, tapering towards the cambium cells; this patterning resembles the same expression pattern observed for PXY. Auxin signalling is mediated by AUXIN RESPONSE FACTORS (ARFs). ARFs are a family of functionally distinct DNA-binding auxin responsive factors. They are likely components that confer specificity to response by auxin through a selection of target genes as transcription factors. One such is that of the PLETHORA genes that are transcribed in response to auxin accumulation and dependent on such ARFs (Aida et al., 2004). Genetic studies have implicated various ARFs in distinct developmental processes through loss-of-function mutational analysis.

### Aims and Objectives

This thesis will further explore and test for genetic interactions that underpin the vascular developmental process in *Arabidopsis thaliana* stems, and the transition from primary to secondary growth in roots. To further understand the molecular and genetic interactions

underpinning vascular development, and the control of secondary growth, a cell type analysis of mutants in the *PXY* and *ER* gene families was undertaken in *Arabidopsis* stems. Quantitative analysis of cell types and the resulting changes to cellular organisation and size were performed. To further explore the mechanisms that regulate secondary growth initiation, in response to RNA sequencing data directed at identifying new candidates that control the transition to secondary growth, the role of the *PLETHORA* gene family was investigated in this process. This work demonstrates that members of the *PLETHORA* family genetically interact with *PXY* signalling genes. Collectively, the results from this thesis show that *PXY* and *ERECTA* combine to regulate vascular development and secondary growth, but that secondary growth is initiated by an interaction between *PXY* and *PLETHORA*.

#### Broader impact of the research

A significant proportion of terrestrial biomass is constituted of xylem cells that make up woody plant tissue (Etchells., 2015). To date, progress in the understanding of the underlying molecular mechanisms and genetic controls that underpin vascular development during secondary growth is incomplete. Application of a fundamental understanding of wood formation could be of importance to biomass industries. Plant biomass represents a large renewable resource of biofuels and biomaterials. This has long been an issue, with significant efforts worldwide by governments and businesses to move towards cleaner renewable energy sources, particularly in Europe and the USA, with meeting the plant biomass targets an obstacle (Somerville, 2006). The ability to manipulate secondary development of xylem, the major component of woody tissue, could increase productivity of commercial forests. Functional genomics of tree species is challenging due to long generation and slow growth times. Production and isolation of genetic mutants for screens is laborious and time consuming. Therefore, the model plant species *Arabidopsis thaliana* is essential for the fast-tracking of the understanding of vascular developmental. Chaffey et al (2002) utilised multiple experimental

approaches to examine the suitability of *Arabidopsis* as a model for wood formation, including histological and cytochemical staining and transmission electron microscopy. They found that the secondary phase of the secondary xylem of *Arabidopsis* closely resembled the anatomy of that found in angiosperm trees. They proposed that *Arabidopsis* can act as a suitable model for answering questions regarding genetic control of cambial growth and secondary xylem development and stated its potential for reverse genetic approaches for genetic identification of orthologues stating that we are confident that comparative genomics between these plants will speed up the identification of the genes responsible (Chaffey et al, 2002). Therefore the work presented here represents a new building element for expansion of current scientific understanding.

## 2. METHODS

### 3.1 Seed stocks

*pxy* and *35S::CLE41 Arabidopsis thaliana* lines used in this study were obtained from laboratory stocks or generated by crossing. *pxf* (*pxy pxl1 pxl2*), *pxf er*, *pxf er erl1*, and *pxf er erl2* lines are described in Wang et al., 2019. *plt3 plt5 plt7* triple mutants were a gift from Ari-Pekka Mahonen.

### 3.2 PCR analysis

*pxy/plt/35S::CLE41* combinatorial mutants were identified in segregating F2 and F3 generations that were obtained from laboratory stocks using PCR analysis. PCR reaction mixtures with a total volume of 15 µL comprised 2 x BioMix Red 7.5 µL (PCR Biosystems); Forward primer (10 µM) 0.5 µL; Reverse primer (10 µM) 0.5 µL; H<sub>2</sub>O 5.5 µL and DNA template 1.0 µL. PCR was performed using standard conditions. Lines with homozygous mutations in the *pxy* gene which also carried a loss of function mutation in *plt3*, *plt5* or *plt7*, either individually or in combination were retained for phenotypic analysis. All loss of function lines carried T-DNA insertions, thus homozygotes were selected on the basis of negative PCR results for gene specific primers but a positive result for those reactions carrying a T-DNA insertion. Primers are detailed in table 1. *35S::CLE41* lines were chosen on the basis of a visual phenotype of extensive cellular proliferation and loss of organisation.

Primer name	Primer sequence
PLT3-1_SALK_F	CACTACCACCCATCTCTGAAAAC
PLT3-1_SALK_R	GCTGATACGTTTGGTCAAAGG
SALK_LBb1	GCGTGGACCGCTTGCTGCAACT
PLT5_SALK_F	TGAAATGATTACCCAACCGTG
PLT5_SALK_R	TAGGCATTAGTCCACCCACAG
PLT7_SAIL_F	GCCTTGACCCTAATCAAATCC
PLT7_SAIL_R	AGCAACTGTTGTTGTTGGAGG
SAIL_LB1	GCCTTTTCAGAAATGGATAAATAGCCTTGCTTCC
Salk_LBa1	TGGTTCACGTAGTGGGCCATCG
PXY-3F	CCCCACACAAAAACCATAATG
PXY-3R	AAAAATCGAGAAGCTTGAGGG

**Table 1:** Primers utilised for genotyping of seed lines. Primers obtained from previously publications.



### **3.3 Preparation of media for plant growth**

Arabidopsis roots were analyzed following growth on Murashige and Skoog media (MS).  $\frac{1}{2}$  MS salt was dissolved in water pH was adjusted to 5.8 with KOH, and agar at 1% was added, prior to autoclaving at 120°C for 20 minutes for sterilization purposes. Media was made in bulk for standardization across experiments. For each experiment, MS agar was melted and poured onto agar plates under sterile conditions.

### **3.4 Sowing of plant seeds**

For plant growth, seeds were sterilised in 70% ethanol for three minutes with gentle shaking before washing once with distilled water under the lamina flow hood. Seeds were imbibed at 4°C for 48 hours to promote equal germination.

Seeds were micro-pipetted onto the media, plates were labelled appropriately for storage and identification purposes, sealed with micropore tape to allow air flow and transferred to the growth cabinet (day zero). Growth conditions were set at long day; 16 hours light, 8 hours dark at 24°C. Seedlings were kept in these conditions and untouched before harvesting at 5, 7 and 14 days growth.

### **3.5 Harvesting of plant material**

Harvesting occurred at 5, 7 and 14 days as appropriate for the individual genotypes respectively. The seedlings were cut with a scalpel at just below the hypocotyl and approximately 1 cm below to collect only the upper part of the root tissue. Multiple root samples were aligned, per genotype, in pre-existing containers with angled edges and set in 5% agarose. To ensure that the agarose solution was not overly hot as to disrupt morphology, molten agar was kept at 50 °C. Once set the agar blocks containing the root tissue were trimmed to size.

### **3.6 Preparation for anatomical sectioning**

Root tissue agar blocks were incubated in glutaraldehyde fixative (0.1 M Phosphate buffer; 2.5 % Glutaraldehyde; 0.01 % Triton X-100) under vacuum for 10 minutes. Samples were then left for 4 hours with gentle agitation. 20 minute Ethanol washes were undertaken with gentle

agitation in a series containing 30%, 50%, 75% ethanol. Samples were then washed twice in 95% EtOH with gentle agitation for 1 hour per wash.

Samples were subsequently infiltrated with JB4 solution (Polysciences). Samples were left for 1 hour with gentle agitation in 75 % EtOH 25 % JB4 infiltration solution (1.35g catalyst benzoyl peroxide, plasticized; 100 ml of JB4 solution A); 50% EtOH 50 % JB4 infiltration solution (1 hour); 25% EtOH 75% JB4 infiltration solution (1 hour); 100 % JB4 infiltration solution (1 hour) then finally with two overnight 100% JB4 infiltration solution washes. Gentle agitation was continued throughout the washing process.

### **3.7 Embedding of JB4 samples.**

JB4-infiltrated samples were prepared for embedding following the manufacturers instructions.

Tissue sample blocks were trimmed to fit within the molds and fresh JB4 solution prepared with JB4 solution B (1.35g catalyst benzoyl peroxide, plasticized; 100 ml of JB4 solution A). Parafilm was applied to cover the mold to ensure anaerobic conditions for hardening of the JB4. Samples were left to harden within blocks overnight and further left for 4-5 days to ensure full hardening before sectioning.

### **3.8 Sectioning and visualization JB4 embedded samples**

Blocks were sectioned at 4  $\mu$ M and sections were stained with 0.05% aqueous toluidine blue for imaging purposes for 30 seconds before washing with water. Visualisation was achieved using standard light microscopy.

### **3.9 Quantification of cell numbers**

Cell numbers were taken from within the vascular cambium and were counted manually and ANOVA performed to check for significant differences.

### **3.10 Radii quantification**

The radii of roots across the genotypes were obtained using the software ImageJ from the centre of the vasculature to the edge.

### **3.11 ClearSee for GFP reporter visualization**

For GFP::PIN1, 35S::CLE41 GFP::PIN1 and *pxy* GFP::PIN1 tagged lines, root tissue was aligned and set in 5% agarose as described above. Samples were incubated in 4% Paraformaldehyde (8 g of paraformaldehyde; 200 ml PBS; pH 6.9) under vacuum for 30 minutes. Samples were twice-washed in PBS for 1-2 minutes, prior to being incubated in ClearSee (Xylitol 10 %; Na Deoxycholate 15 %; Urea 25 %) for a minimum of 14 days.

### **3.12 GUS staining and Technovit embedding**

For the GUS reporter lines, root tissue was aligned and set in 5% agarose as described in 3.4. Samples were incubated in 50 mM phosphate buffer for 5 minutes, then treated with ice-cold 90% acetone for 5 minutes, rinsed in 50 mM phosphate buffer, incubated with GUS staining buffer under vacuum for 10 minutes, then incubated at 37°C overnight in fresh GUS staining buffer with X-glucoside. Stained tissue was fixed in FAA (50 % ethanol: 3.7% formaldehyde; 0.5% acetic acid) for 30 minutes at room temperature with gentle shaking followed by a progressive series of EtOH washes for 30 minutes each at 70%; 85%; 95% EtOH. Samples were incubated in Technovit 8000 pre-infiltration solution at room temperature for 90 minutes with gentle shaking. Pre-infiltration solution was removed, and samples were incubated with the Technovit infiltration solution overnight at room temperature. Samples were prepared in molds with Technovit polymerization solution as per the manufacturer's instructions.

### **3.13 Yeast-2-hybrid**

For cloning of cDNA for use in the yeast-2-hybrid, primers for WOX14 and TMO6 were used in 30 µL reactions comprised of; 15 µL Phusion master mix (Thermo-Fisher), cDNA 5 µL, Forward primer (NdeI) 1 µL, Reverse primer (XhoI/PstI) 1 µL and the remaining volume H<sub>2</sub>O (Tables 3-4). PCR products were run on an agarose electrophoresis gel for band separation. UV exposure to identify amplicons was limited to avoid DNA damage. PCR products were excised from the gel and purified.

The products were ligated into the vector pJET following a blunt end cloning protocol comprised of 2X DNA ligase reaction buffer (10  $\mu$ L); PCR product (1  $\mu$ L); pJET 1.2 cloning vector (1  $\mu$ L); T4 DNA ligase (1  $\mu$ L) and up to 20  $\mu$ L H<sub>2</sub>O (nuclease-free). Samples were vortexed briefly and left overnight at room temperature. Ligated vectors were transformed in to competent *E. coli* using heat shock treatment at 42 °C, and grown in liquid broth (LB media) for 1 hour, then plated on to carbenicillin selection plates to select for the carbenicillin resistance gene in the pJET vector. Identification of successful plasmid transformations were performed through PCR reactions with pJET 1.2 forward and reverse primers in 20  $\mu$ L total mixtures; 2X BioMix red (PCR Biosystems; 7.5  $\mu$ L); pJET 1.2 forward primer (0.5  $\mu$ L); pJET 1.2 reverse primer (0.5  $\mu$ L); Colony DNA (suspended bacteria scraped from individual colonies on the selection plates and suspended in H<sub>2</sub>O; 1  $\mu$ L); H<sub>2</sub>O (5.5  $\mu$ L). Successful transformation of the pJET plasmid in to the *E. coli* colonies was confirmed by the presence of a band by PCR. Distinction between WOX14 and TMO6 was achieved through the identification of a product of appropriate size of the bands produced. Positive colonies were grown in liquid LB media at 37 °C with 200 rpm shaking. *E. coli* cells from the liquid colonies were lysed and the plasmid DNA was purified on a Miniprep column (Qiagen) as described in the manufacturer's instructions. Sequencing was performed utilising the pJET forward and reverse primers and aligned utilising the Benchling online application tool (Benchling.com).

After confirmation of successful cloning, plasmids were cut at the restriction enzyme sites, using NdeI, PstI and XhoI. Conditions for restriction enzymes were determined according to information from the supplier's website (ThermoFisher), with all three enzymes had a working temperature of 37 °C. Reactions were set up in 15  $\mu$ L reactions with alkaline phosphatase to prevent self-annealing in subsequent steps. Reactions were comprised of; orange buffer (1.5

μL); DNA (500 ng); NdeI (1.5 μL); XhoI/PstI (1.5 μL); FastAP (only in vector restriction digest; 1.5 μL); H<sub>2</sub>O to bring volume up to 15 μL.

The restriction digest mixtures were gel-purified. Products were ligated in to the restricted vectors respective to the complementary digested ends; NdeI-WOX14-XhoI to the NdeI-PGAD T7-XhoI vector and NdeI-WOX14-PstI to the NdeI-PGBK T7-PstI vector as with TMO6 respectively. Ligation mixtures ran overnight on the bench. Ligation reactions in total volumes of 10 μL contained 10X DNA ligase buffer (1 μL); Yeast II hybrid vector backbone (PGAD t& digested/PGBK T7 digested) 4 μL; Transcription factor cDNA (TMO6/WOX14 digested) 4 μL and T4 DNA ligase 1 μL. Ligated mixtures were transformed through the transformation process for uptake into competent *E. coli* cells, and plated on selection plates containing carbenicillin for pGAD T7 and kanamycin plates for pGBK T7 vectors. Following confirmation of positive colonies by PCR, plasmids were maintained as glycerol stocks.

LEFT	5' CTCATTGTCTTGTTTCATATGGTAAA 3'
RIGHT (XhoI)	5' [CTCGAG]TCTATACGAATTTTAAGTCTCCA 3'
RIGHT (PstI)	5' [CTGCAG]TCTATACGAATTTTAAGTCTCCA 3'

*Table 2: Primer designed for WOX14. [] brackets indicate inclusion of restriction enzyme sites.*

LEFT	5' CATATGGATCATTTGTTACAACACCAGGATGT 3'
RIGHT (Xho1)	5' [CTCGAG]CATAAATAGCTACCACCCTTTCTACTCC
RIGHT (Pst1)	5' [CTGCAG]CATAAAATAGCTACCACCCTTTCTACTCC 3'

**Table 3:** Primers designed for TMO6. [] brackets indicate inclusion of restriction enzyme sites.

### 3. ERECTA STORY; VASCULAR DEVELOPMENT IN THE STEM

#### Background

Work from this chapter is included in the publication, Organ-specific genetic interactions between paralogues of the PXY and ER receptor kinases enforce radial patterning in Arabidopsis vascular tissue (2019). Ning Wang, Kristine S Bagdassarian, Rebecca E Doherty, Johannes T Kroon, Katherine A Connor, Xiao Y Wang, Wei Wang, Ian H Jermyn, Simon R Turner, and J Peter Etchells. Development **146**: dev. 177105.

Mutations in the *PXY* gene have been shown to demonstrate reductions in vascular cell number and vascular organisation (Etchells et al., 2015). Via a genetic interaction, the PXY signalling module has been linked with a second ligand receptor pair. The leucine rich repeat ERECTA (ER) receptor is phloem expressed (Uchida et al., 2013) and its cognate ligands CHALLAL-LIKE2/EPIDERMAL PATTERNING FACTOR-LIKE4 (CLL2/EPFL4) and CHALLAH (CHAL/EPFL6) are expressed within the endodermis (Abrash et al, 2011; Uchida et al, 2012). Plants carrying mutations in both PXY and ER show defects in the organisation of the vasculature that are greater than those observed in single *pxy* mutants, but no enhancement of the *pxy* vascular proliferation defects were observed in *pxy er* plants. *er* single mutants have a phenotype very similar to that of wild type in the inflorescence stem vascular tissue. This indicates genetically separable outputs between cell division and vascular organisation (Etchells et al, 2013).

Within the Arabidopsis genome, paralogues of ERECTA exist. These are ER-LIKE1 (ERL1) and ER-LIKE2 (ERL2) (Shpak et al, 2004). The ERECTA family (ERf) are acknowledged as having various roles within the regulation of plant growth and development. They act redundantly to regulate cell elongation, cell division, inflorescence architecture (Shpak et al,

2004; Torii et al, 1996), shoot and apical meristem fate (Kimura et al, 2018; Uchida et al, 2013) amongst other roles. In the context of vascular development, ERF regulates vascular expansion in the stem (Uchida et al., 2013) and hypocotyl through control of xylem fibre formation timing, and levels of radial growth (Ikematsu et al, 2017, Ragni et al, 2011). A characteristic of loss of ERF genes is an increase in cell size, with particular respect in the radial axis (Shpak et al, 2004; Shpak et al, 2003). PXY also has two paralogues in Arabidopsis, PXL1 and PXL2 (Fisher & Turner, 2007), collectively referred to as PXf for *PXY*-family.

### **Aims and objectives**

To determine if PXY and ER paralogues interact to regulate vascular development, genetic relationships between PXf and ERF receptors were investigated. Analysis of the *pxy pxl1 pxl2 er erl1 erl2* sextuple mutants and their parental lines that had previously been created using a combination of classical genetics and genome editing was undertaken. Analysis of these lines demonstrated that PXf and ERF genetically interact to coordinate tissue integrity at the levels of both cell size, and cell division. These results demonstrate that interactions between members of both families are critical in patterning of vascular tissue in the stem.

### **Results**

#### **Phenotypic results of *pxf erf* sextuple mutants**

To test whether PXY-like and ER-like genes contributed to vascular development, *pxf*, *pxf er*, *pxf er erl1*, *pxf er erl2*, and *pxf erf*, vascular tissue in the inflorescence stem was analysed. Thin sections were taken from stem tissue of 5-week-old plants with histological microscopy imaging facilitating cell counting. Vascular morphology was similar in *pxf erf* lines and *pxf er erl2* counterparts. Both were characterised by very large reductions in vascular bundle size. Characteristic xylem and phloem cell types were present, but only very small xylem vessels were observed, relative to those found in wild type, *erf* and *pxf* lines (Figures 7D-E, 8A). Tissue



layer organisation defects were also apparent beyond those observed in control lines. The clearly defined organisation of endodermal and adjacent phloem cap cells were lacking as the phloem cap appeared to extend into the cortex (Figure 7D) or be absent altogether (Figure 7E). Thus, tissue layer defects occurred out with vascular cell types. These similarities in vascular morphology were independent of plant size because gross morphology of *pxf erf* sextuple lines was considerably smaller than *pxf er erl2* counterparts.

### **Quantitative morphology of PXf and ERf mutant combinations**

Analysis of *pxf er erl2*, and *pxf erf* lines suggested that these genes coordinate cell size because xylem vessels in these stems appeared small (Figure 7A). Consequently, cell morphology of vascular cell types was determined from the transverse sections (Figure 7). To capture measurements for the cell perimeters and areas, images from 6 different individuals were selected for each genotype tested. A minimum of 10 cells of each cell type (xylem vessels, xylem fibres, and phloem) were selected. Cells of each type were selected along the full length of the radial axis to ensure that cells of all sizes and phenotypic variation were represented. For each cell type, an equal number of cells was selected on a random basis from each plant within each genotype to avoid small variations between the number of representatives obtained from each individual plant. A MATLAB code was generated to extract the intrinsic properties of each cell type (Bagdassarian et al, 2020). To test the significance of the variation between the cell areas and perimeters between the different genotypes, a nested ANOVA was performed with a Tukey HSD post-hoc test.

In stems, xylem vessels and cells in the phloem were smaller in *pxf* lines than wild type, as determined by measuring both cell perimeter and cell area. Removing *ER* from *pxf* lines resulted in no change to the size of these cells, but loss of *ERL2* from *pxf er* plants caused a further reduction in cell size (Figure 8A, C). Thus, in phloem and xylem vessels *pxf* and *erf*

families interact to maintain cell size. Xylem fibre sizes differed from this trend. Here, *pxf er* cells were significantly larger than wild type, but this phenotype was suppressed in *pxf er erl2* plants as fibre perimeter and area was unchanged from wild type (Figure 7B). We were unable to assess fibre morphology in *pxf erf* vascular bundles as too few were identifiable in these lines (Figure 7E). Taken together, our results demonstrate that a genetic interaction between PXf and ERf signalling coordinates organ size at the level of cell size, in addition to those of proliferation, and pattern maintenance in both stems and hypocotyls.

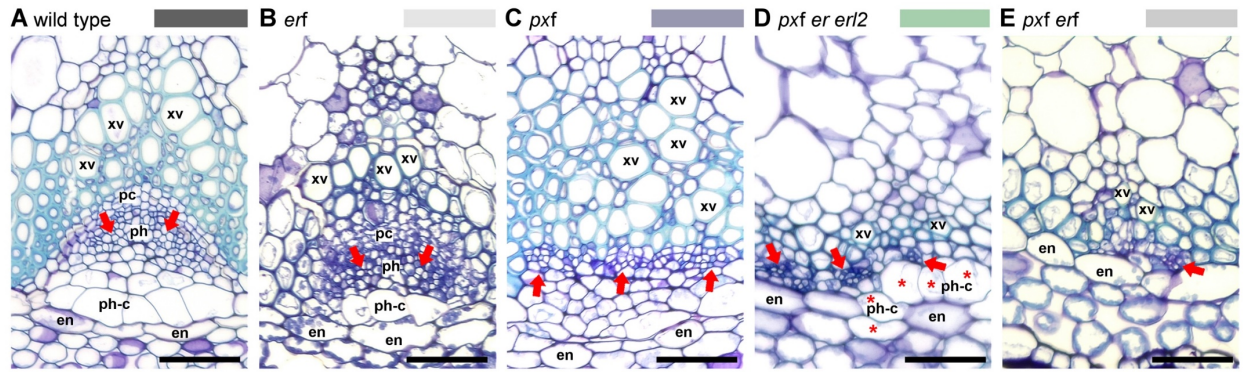


**Figure 7:** Stem tissue from *pxf erf* lines showing the vascular bundles across genetic lines and the identification of cell types utilised for calculating cell size. (A) Wild-type, (B) *erf*, (C) *pxf*, (D) *pxf erf erl2*, (E) *pxf erf* vascular bundles. Phloem arrangement is marked with red arrows. Cells with phloem cap-like morphology are marked with asterisks. Scale bars: 50  $\mu$ m; xv, xylem vessel; pc, procambium; ph, phloem; ph-c, phloem cap; en, endodermis.

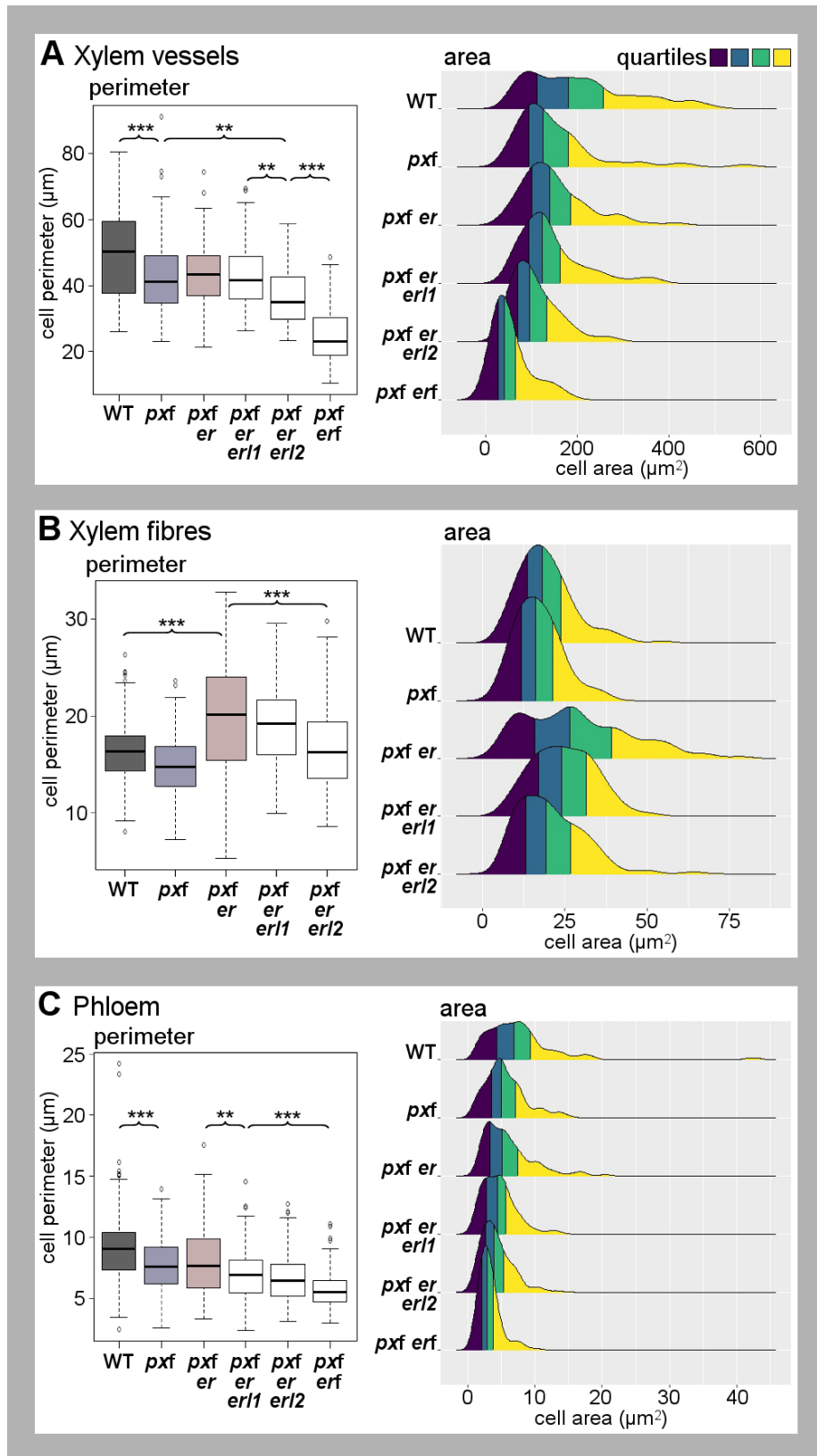


**Figure 8:** Comparisons of morphology of cells in stem vascular bundles. (A-C) Boxplots on left show mean cell perimeter for xylem vessels (A), xylem fibres (B) and phloem cells (C). Boxes represent the 25th to 75th percentile, the horizontal line marks the median. Whiskers' endpoints are the min/max points within the interval spanning  $Q1-1.5*IQR$  (lower) and  $Q3-1.5*IQR$  (upper). Asterisks mark significant differences (ANOVA plus Tukey; \*\*\* $P < 0.001$ , \*\* $P < 0.01$ ; J Ridgeline plots on the right show the distributions of cell areas divided into quartiles. Areas of pxf er lines were greater than those of pxf er erl2 lines in all three cell types ( $P \leq 0.05$ ). Differences were calculated with ANOVA and a Tukey post-hoc test.

## Discussion

Evidence that mechanisms exist to adjust cell morphology in order to maintain tissue size and organisation include the observation that cell expansion differs according to the rate of cell division. Here, overall organ size in mutants with fewer cells is often comparable to or only subtly different from those of wild-type plants due to an increase in cell size (De Veylder et al., 2002; Hemerly et al., 1999; Shpak et al., 2004; Ullah et al., 2001). We found that the interaction between *PXf* and *ERf* was crucial to regulation of cell size in multiple cell types. The ability to adjust cell size to compensate for the profound reductions in cell division in *pxf er* lines was particularly dependent on *ERL2*. This is in contrast to the consequences of losing the *ERECTA* family alone, as cell size adjustments are a feature of *erf* mutants (Shpak et al., 2004). However, the influence of *ERL2*, *ER* and *ERL1* differed by cell type and organ. In stem vascular bundles, the only cell type with an increase in size in response to fewer to cell divisions were the fibres. This phenotype was suppressed by removal of ERL genes. These observations support the idea that one function of the genetic interaction between *ERf* and *PXf* is coordination of tissue expansion. We propose that with these signalling mechanisms removed, the positional information that must be interpreted for cell morphology adjustments to occur is missing, highlighting the fundamental signalling role.

## 4. SEEDLING STORY; THE INITIATION OF SECONDARY GROWTH

### Background

Factors controlling the transition to secondary growth in *Arabidopsis* hypocotyls have recently been described. It first arises in cells adjacent to xylem, and central to this transition is an accumulation of auxin and expression of *HD-Zip III* transcription factors. These factors, in turn, activate expression of *PXY* signalling (Smetana et al., 2019). Nevertheless, *pxy* mutants, and indeed *pxf* triple mutants, do ultimately make the transition to secondary growth. Thus, other factors must act with *PXY* to regulate the transition to secondary growth and radial pattern in hypocotyls. *pxy erf* double mutants, *erf* triple mutants, *pxf erf* quads, and both *pxf erf1* and *pxf erf2* quintuple lines all made the transition to full secondary growth. By contrast, *pxf erf* sextuple mutants do not, supporting the idea that these receptor families coordinate development through a genetic interaction, and that the phenotypes cannot be explained simply by a correlative loss of cell division-promoting factors (Wang et al., 2019). How *PXY* (and *ER*) signalling regulate the transition to secondary development in the vascular tissue is currently not known. However, the process by which higher plants organise their vascular tissue is underpinned by several molecular and genetic pathways. The emergence of these pathways led to one of the most important evolutionary adaptations of higher plant species; the ability to populate land (as discussed in Lucas et al., 2013). Vascular development occurs in four main processes; specification, establishment, maintenance and differentiation (Rybel & Mähönen et al, 2015). Early establishment of the root vascular tissue has been linked to growth and patterning and is specified by a hormone signalling network that includes phytohormones and transcription factors (Rybel & Mähönen et al 2015). One possibility is that these pathways become repurposed to control initiation of secondary growth later in development.

Auxin is a major coordinating signal of plant development. Predominantly auxin takes the form of indole-3-acetic acid (IAA), with much of its developmental influence dependent on differential distribution within the plant tissues and the formation of local maxima or auxin gradients (Petrášek & Friml, 2009). In addition to induced local biosynthesis and the release of active forms from inactive precursors, the major determinant of differential auxin distribution is the directional transport and flow between cells (Petrášek & Friml, 2009). Intracellular auxin movement relies upon several auxin-transporting mechanisms. These include both passive and active forms of transport over both long and short distances across the plant. Most auxin is transported across a gradient via bulk phloem transport from source tissues (young leaves and flowers). In addition, there is regulated carrier-mediated cell-to-cell directional transport within the vascular cambium from the shoot towards the root apex (Goldsmith, 1977). The major mechanism reported within the literature is movement facilitated through membrane-bound auxin influx and efflux carriers. One family identified as influx carriers are the AUX1/LAX family. *auxin resistant 1 (aux1)* mutants showed resistance to exogenous stimulation by synthetic auxin and were identified as a family of transmembrane proteins similar to amino acid permeases (Bennett et al, 1996; Swarup et al., 2008). Identification of auxin efflux carriers was via investigation of several mutants of Arabidopsis including *agravitropic 1 (agr1)*, *wavy roots 6 (wav6)* (Bell & Maher, 1990; Okada & Shimura, 1990), *ethylene insensitive root 1 (eir1)* (Roman et al, 1995) and the floral mutant *pin-formed1 (pin1)* (Okada et al, 1991). The *pin-formed* mutant *pin1-1* has structural abnormalities in the inflorescence axes, flowers and leaves. The loss of function mutant can result in the loss of stamens, wide petals, pistil-like structures with no ovules and the loss of floral buds in the axes. An independently isolated allelic mutant *pin1-2* also showed similar loss-of-function phenotypes. The loss of function mutant phenotypes are replicated in wild-type plants cultured in the presence of chemical auxin polar

transport inhibitors 9-hydroxyfluorene-9-carboxylic acid or N-(1naphthyl)phthalamic acid (Okada et al, 1991). Okada et al tested for polar transport activity in the loss of function mutants, showing a decreased activity of 15% and 7% comparative to wild type (untreated). They suggested the polar transport is required within the early developmental stages of the floral bud formation in Arabidopsis and that the primary function of the *PIN 1* gene is auxin polar transport in the inflorescence axis.

PIN1 belongs to the PIN-FORMED (PIN) protein family of secondary transporters acting in the efflux of auxin (Kreček et al, 2009). Typically, these proteins are asymmetrically localised within the cell, and their distribution determines the directionality of intercellular auxin flow. PIN genes are found exclusively in the genome of multicellular plants and underpin the key developmental stages of embryogenesis, organogenesis, tissue differentiation and tropic responses (Kreček et al, 2009). The expression of the PIN family in relation to incipient cotyledons (growing embryonic leaf) in embryos results in the formation of two cells at the centre of the embryo receiving higher auxin concentrations comparative to the other cells, thus defining the provascular initials (Reinhardt et al. 2003). Auxin is perceived by the SCF (SKP1-CUL1-F-box) ubiquitin ligase triggering the degradation of Aux/IAA transcriptional inhibitors. This leads to the activation of DNA-binding AUXIN RESPONSE FACTORS (ARFs) (Rybel & Mahonen, 2015). The ARF5 transcription factor MONOPTEROS (MP) is critical for the formation of the provascular tissue in response to the PIN-derived auxin maxima. Mutations in *MP* lead to very early division defects in the provascular initial cells.

In terms of the early establishment of root vasculature during embryogenesis many regulatory components have been identified. These include auxin response factors such as ARF5, TMO5 (TARGET OF MONOPTEROS 5) and LHW (LONESOME HIGHWAY) of which loss of



function results in reduced periclinal divisions (De Rybel, B. et al. 2013; Ohashi-Ito & K. & Bergmann, 2007; Ohashi-Ito, Matsukawa & Fukuda, 2013.), AHK4/CRE1 (ARABIDOPSIS HISTIDINE KINASE 4) a cytokinin receptor (Mähönen et al. 2000; Mähönen et al., 2006), AHP6 (ARABIDOPSIS HISTIDINE PHOSPHOTRANSFER PROTEIN 6) (Mähönen et al. 2006) which is a negative regulator of cytokinin signalling and also MONOPTEROS as a target gene (Bishopp et al., 2011).

### **Aims and objectives**

While the developmental regulators above describe regulation of primary vascular tissue development, essentially only three components are known to regulate the transition to secondary growth; PXY-ER and their paralogues, HD Zip III transcription factors, and auxin. To identify further candidates, wild type, *pxy*, and *35S::CLE41* lines were separated in to root and shoot tissue at 7 days old, which corresponds with the onset of secondary growth, and subjected to RNA-seq. This unpublished data from the Etchells lab provided insights into further regulators of this process. At the 7 day time-point, *pxy* mutants had not yet started to initiate secondary growth, but these divisions had occurred in wild type hypocotyls, and more prominently in *35S::CLE41* (lines which signalling through PXY is increased due to higher expression of TDIF precursors; figure 9 A-D).

Given a set of genes that are mis-expressed under certain conditions a Gene Ontology (GO) enrichment analysis will identify statistically significant annotation terms that are over or under-represented for that gene set. GO terms cover cellular components, molecular functions and biological processes, with lower levels of GO terms applied to genes when relevant (Zhou et al, 2007). Here, the RNA-seq data from 7 day old Arabidopsis seedlings were analysed enriched categories.

Enriched GO categories included increased responses to water, water deprivation and desiccation (not shown). These results were not unexpected due to the primary function of the vascular tissue, and xylem in particular acting to transport water. Any defects that control vascular development and function will affect water transport, so this data supports the idea that the RNA-seq data is a true representation of perturbations to gene expression. Specific GO ontologies likely to be characteristic of changes to plant development, for loss of *PXY* (shown in figure 9E) or an increase in signalling through PXY (*35S::CLE41*; shown in figure 9H) were identified. Changes to the pathways of two previously mentioned phytohormones, auxin and cytokinin were observed in these data sets, supporting their putative role in secondary growth initiation. To identify key genes of interest, differentially expressed genes that were oppositely regulated in *35S::CLE41* lines compared to *pxy* mutants were identified (Figure 9F). Genes identified by this approach expectedly included both the *PXY* gene itself, and *CLE41* thus validating this approach. Three other genes that will form the basis of enquiry for this thesis were also identified based upon changes to their expression highlighted through the study. These were *PLT3*, *PLT5*, and *WAG2*.

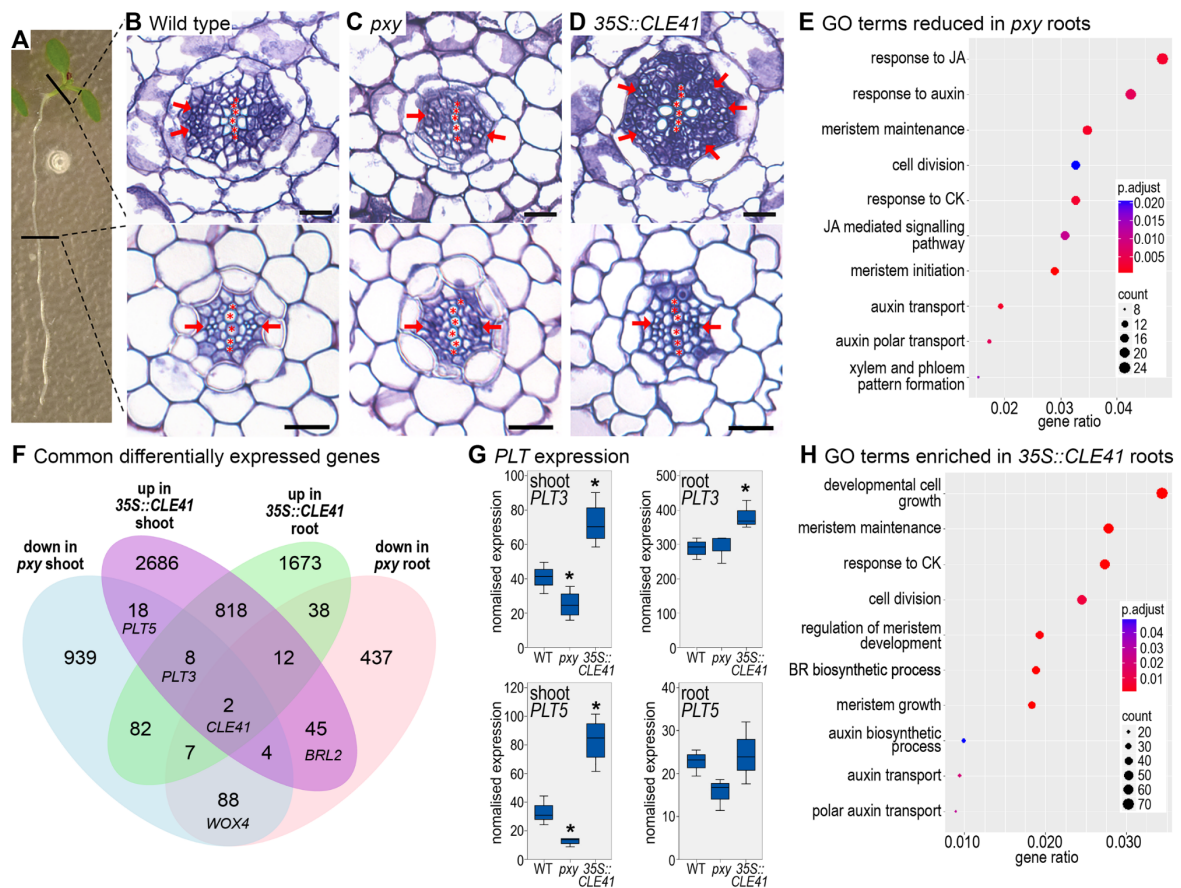


**Figure 9:** GO Analysis data utilised for identification of target genes. (A) shows a 7 day old *Arabidopsis* seedling and the locations of cut sections on the hypocotyl and root. (B-D) Show horizontal cross sections of the respective sections (upper row from the hypocotyl and lower row from the root). The xylem pole axis is indicated with the asterisks and the phloem poles indicated by the red arrows. This shows the increase in cellular proliferation as observed in the overexpression 35S::CLE41 background, and lack of cellular proliferation in pxy. (E & H) Show gene ontology analysis of two of the comparisons from the RNA-seq data. This identifies key gene categories. (F) Shows a Venn diagram used to identify genes that were mis-expressed in multiple data sets. PLT genes are marked (with a couple of others as identified for further explorative study within this thesis.). (G) Shows the normalised gene counts for PLT genes from the RNA-seq data.

### The Plethora story

The WAG2 gene in *Arabidopsis* encodes a protein serine/threonine kinase that is homologous to genes within the PINOID family. It acts as a positive regulator of cellular auxin flow. WAG2 has been found to regulate organ development through the enhancement of PIN-mediated polar auxin transport. Localisation of WAG2 correlates with the apical localisation of PINs (Dhonukshe et al., 2010). Dhonukshe et al found that WAG2 acted to regulate embryo development and adaptive root development and that the PID and WAG protein kinases acted redundantly to regulate PIN polarity during cotyledon and root development (Dhonukshe et al., 2010). Studies on PIN polarity identified the ability of WAG2 to phosphorylate PIN. Identification of varied expression of this gene through RNA-seq analysis led to explore the localisation of PIN proteins in response to changes in *PXY* signalling.

The genes PLT3 and PLT5 belong to the gene family PLETHORA, or alternatively referred to as the AIL (AINTEGUMENTA-LIKE) family, which were originally identified as essential regulators controlling stem cell activity within the root (Aida et al., 2004; Santuari et al., 2016). In *Arabidopsis* roots, aspects of the process of zonation, the generation of three distinct developmental zones, are co-controlled by auxin and PLT transcription factors. Whilst PLT is transcribed in correlation to high auxin accumulation, iterative experimental and computational approaches have shown that the PLT gradient is not a direct, proportionate readout of the auxin gradient (Mahonen et al, 2014). Prolonged high auxin levels generate a narrow PLT transcription domain from which a gradient of PLT protein is subsequently generated. The resulting levels of PLT defined the location of three root developmental zones (Mahonen et al, 2014). PLT genes are also key effectors for establishment of the stem cell niche during embryonic pattern formation (Aida et al., 2004).

Further, the patterning of plant organ initiation at the SAM is a process termed phyllotaxis incorporates the phytohormone auxin alongside PIN auxin efflux proteins. Organ initiation is associated with the polarisation of PIN proteins and auxin accumulation (Okada et al, 1991; Galweiler et al, 1998; Reinhardt, 2000; Benkova et al, 2003; Heisler, 2005; de Reuille et al, 2006; Jönsson, 2006; Wisniewska et al, 2006). It has been shown that three PLT-like AP2 domain transcription factors also act redundantly to control shoot organ positioning (Prasad et al, 2011). The loss of function in *plt3*, *plt5* and *plt7* lead to the non-random, metastable changes in phyllotaxis, largely attributable to a mis-regulation of the PIN1 protein. The defects were able to be recapitulated by reducing PIN1 dosage, revealing PLT proteins as key regulators in phyllotaxis control by PIN protein regulation.

Whilst PLT genes have been shown to be key regulators of PIN protein localisation in other developmental stages and processes of Arabidopsis, their role within secondary development, in particular in their ability to drive division in the cambium is not known. The cambium zone of poplar stems has been observed to retain the highest concentration of auxin (Bhalerao & Fischer, 2014). Mutant plants with reduced sensitivity to auxin, such as auxin responsive factor 1 (*ARF1*), exhibit lower activity of interfascicular cambium (Agusti et al., 2011). PIN proteins in the surrounding tissues promote cambium activity by increasing the auxin concentration, as dependent on the localisation of such PIN proteins. It remains to be determined whether *PLT* gene expression is subject to the auxin maxima in the cambium.

### **Aims and objectives**

A change in auxin distribution has recently been described as the driving switch from primary to secondary growth (De Rybel et al., 2015). However, the molecular and genetic mechanisms that facilitate this change in auxin distribution are not known. One possibility is that PXY signalling may regulate this redistribution. The transition to secondary growth is late in *pxy* mutants and plants with *CLE41* overexpression transition early. The RNA-seq data discussed

previously was performed at a time that correlated with this transition from primary to secondary growth and auxin distribution changes. Auxin is transported by PIN proteins, and phosphatases of the PINOID family dictate where PIN proteins are localised within the cell. Expression of PINOID gene family member WAG2 was reduced in the loss of function *pxy* line and increased in the transgenic 35S::*CLE41* line. This leads to a hypothesis whereby secondary growth could be initiated by PXY signalling which in turn influences the localisation of PIN proteins that generate auxin distribution. Localisation changes in PIN proteins could, in part, be responsible for the transition secondary growth. Such a hypothesis would be supported by the upregulation of PLT transcription factors that under some circumstances respond to auxin levels.

## Results

We hypothesised that the *PLETHORA* genes lie down stream of PXY signalling. This was tested through a genetic study. Crosses of the *plt3 plt5 plt7* mutant lines to *pxy* and 35S::*CLE41* had been undertaken previously, but no homozygous lines had been identified. Selection of such lines was performed in segregating F2 populations. The aim was to identify plants with higher order loss of function mutations within the *plt3* and *plt5* genes in both *pxy* loss of function and 35S::*CLE41* over expression backgrounds. Plants were selected by genotyping. Genomic DNA extraction followed a CTAB extraction methodology, genotyping was performed PCR. *pxy plt3 plt5* and 35S::*CLE41 plt3 plt5* lines were identified which were then compared to WT, *pxy*, 35S::*CLE41*, and *plt3 plt5 plt7* controls to determine if there were changes to vascular development.

Plants were grown on MS agar under sterile conditions. The upper region of their root tissue just under the hypocotyl was examined at 5, 7, 14 and 28 days. Sections of tissue were stained with toluidine blue and visualised utilising standard microscopy techniques to compare

phenotypes Figures 10-12 show the cross-sectional images across the individual genotypes for qualitative comparison. They show specific time points across the root growth and transition from primary to secondary growth. Shown are the morphological differences as a result of genetic mutations in the *PXY* signally pathway. Shown are losses to cellular proliferation and organisation within the vasculature, with enhancement and suppression of mutant genotypes under multiple gene mutations.

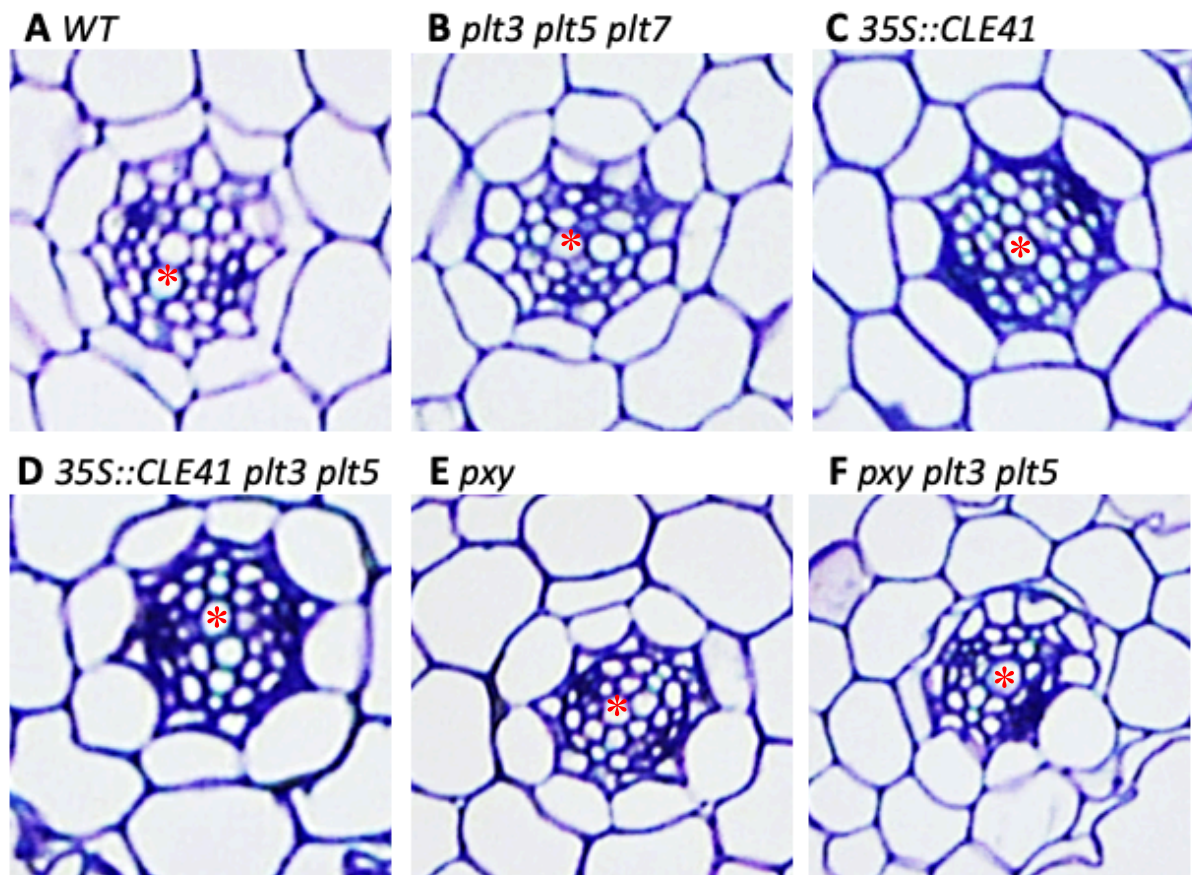


**Figure 10:** Transverse cross sections taken at 7 days of growth of the *Arabidopsis* seedling root. Sections are stained with Toluidine-blue. The primary xylem initials are marked by red asterisks. Little qualitative morphological differences of significance observed between genotypes.



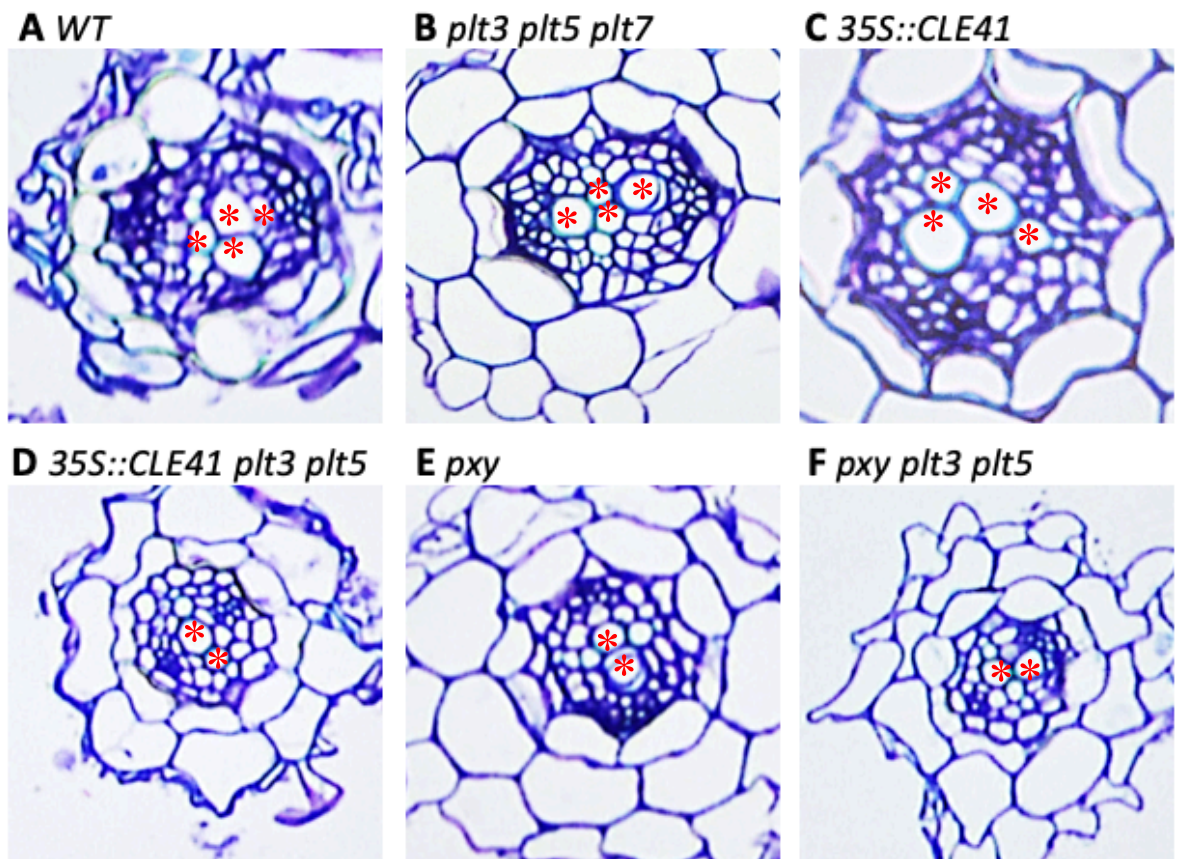


**Figure 11:** Transverse cross sections taken at 14 days of growth of the *Arabidopsis* seedlings. Sections are stained with Toluidine-blue. The primary xylem initials are marked by red asterisks. Little qualitative morphological differences of significance observed between genotypes.

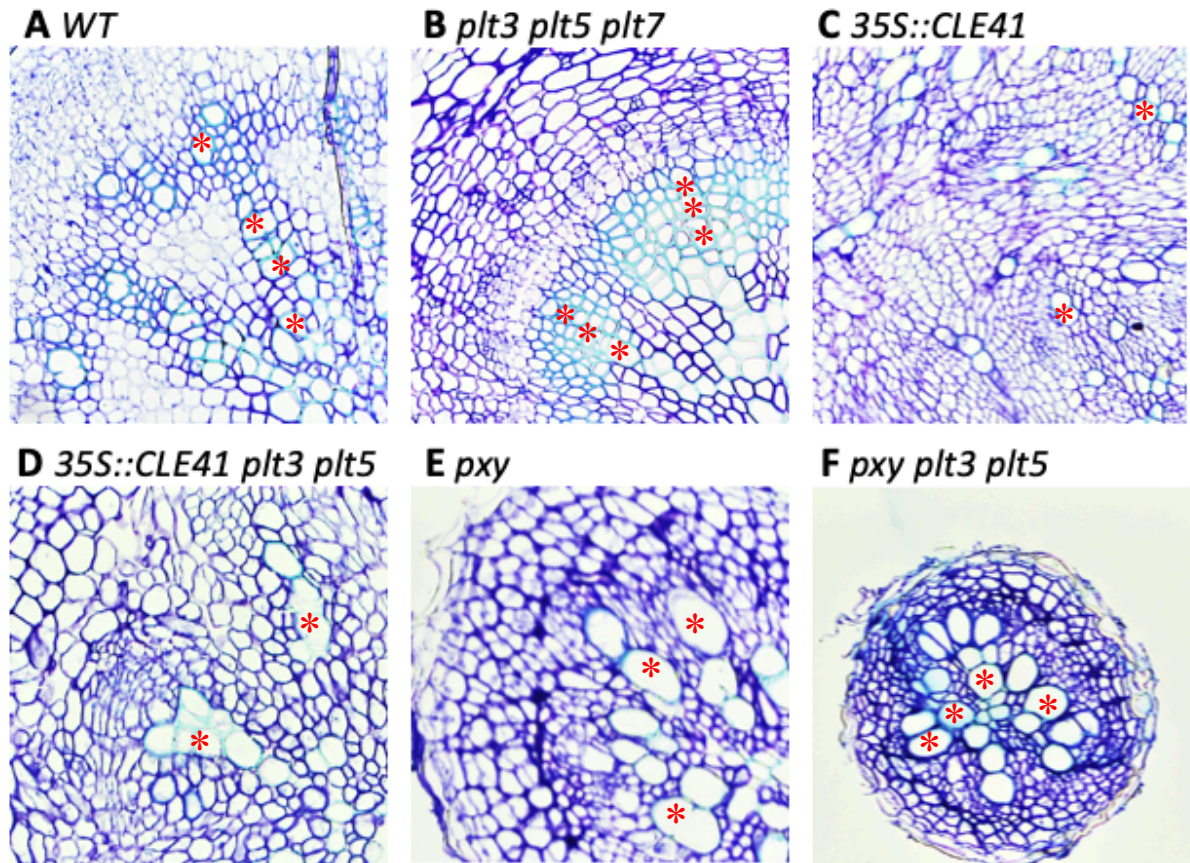


**Figure 12:** Transverse cross sections taken at 28 days of growth of the *Arabidopsis* seedlings. Sections are stained with Toluidine-blue. There are obvious morphological differences between genotypes at this stage, when secondary growth is well established. There is distinct loss of organisation within the 35S::CLE41 overexpression backgrounds. In *pxy* mutation backgrounds there also is an overall size reduction of root radii. The *pxy plt3 plt5* shows a clear enhancement of the *pxy* phenotype in (F). There is a suppression of cell proliferation in the 35S::CLE41 background shown in (D) comparative to (C) and (A). Xylem cells or cell bundles are marked by red asterisk.

### Genetic interactions between *PXY* signalling and *PLT* genes

The transition from primary to secondary growth occurs at roughly 7 days of growth. Therefore, up until this transition, there was a lack of different phenotypes between the loss of function mutations and the overexpression lines assuming that the role of these genes was confined to secondary development, this was as expected from the hypothesis. Before the initiation of secondary growth, the vascular procambium is present between primary phloem and xylem (Figure 10). At 7 days, the *pxy* mutant line did not differ in phenotype from that of either *35S::CLE41* or the WT. Furthermore, the *plt3 plt5 plt7*, *pxy plt3 plt5* and *35S::CLE41 plt3 plt5* lines also showed no deviation from WT. No changes at 7 and 14 days was supported by quantitative analysis. Determination of cell number in the vascular cylinder at these time points led to the conclusion that there was no quantitative change. No significant differences between any of the genotypes was observed.

At 28 days, the transition to secondary growth has been initiated and was well established. Here, differences between the genotypes were observed. No phenotypic deviation was observed between WT and the *plt3 plt5 plt7* mutant. The overexpression line, *35S::CLE41* however, had enhanced cell division, and the *pxy* mutant appeared smaller (Figure 12), as has been previously described. The *pxy plt3 plt5* mutant shows an enhancement of the *pxy* phenotype. There was very little cell division and xylem and phloem appeared adjacent, rather being separated by a clearly defined cambium (Figure 12), thus the vascular cambium appeared further reduced in size. The *pxy plt3 plt5* mutant retained the organisational defects that are characteristic to the *pxy* mutant, loss of organisation with the phloem cells intercalated with those of the xylem and size reduction yet shows an enhancement in regard to the loss of cell proliferation.

Of note here, was the phenotypic changes caused by *plt3* and *plt5* mutations in the *35S::CLE41* background. The typical escalation of cell proliferation that is characteristic of *35S::CLE41* was partially masked by *plt3* and *plt5* loss of function mutations (Figure 12D). The *35S::CLE41 plt3 plt5* mutant shows a suppression of the overexpression phenotype. There was a clear reduction in the number of undifferentiated cells comparative to the *35S::CLE41* control, as seen by the presence of groups of xylem vessels. Such groups were absent from *35S::CLE41*, but present in *35S::CLE41 plt3 plt5* (Figure 12).

Difference between genotypes were determined using quantitative methods. ImageJ software was used to determine the radius of the roots (Figure 13). Whilst the n was low and is perhaps the reason for no differences between WT, *pxy* or *35S::CLE41*, an ANOVA plus a posthoc-Tukey test was used to identify a significant difference between *35S::CLE41 plt5* and *35S::CLE41 plt5 plt3* genotypes. One explanation for the increase in size of *35S::CLE41 plt5* relative *35S::CLE41* could be that *35S::CLE41 plt5* lines demonstrate higher levels of cell differentiation (differentiated cells in the xylem are larger than cambium cells), but in *35S::CLE41 plt3 plt5* lines, the proliferation was also reduced. While this requires further investigation, the xylem number was indistinguishable between these three genotypes, these results support the idea of redundancy between *PLT3* and *PLT5*. This was supported by counts of xylem cell number which were reduced in *pxy plt3 plt5*, but not in *pxy plt5*, *pxy*, or *plt3 plt5 plt7*.



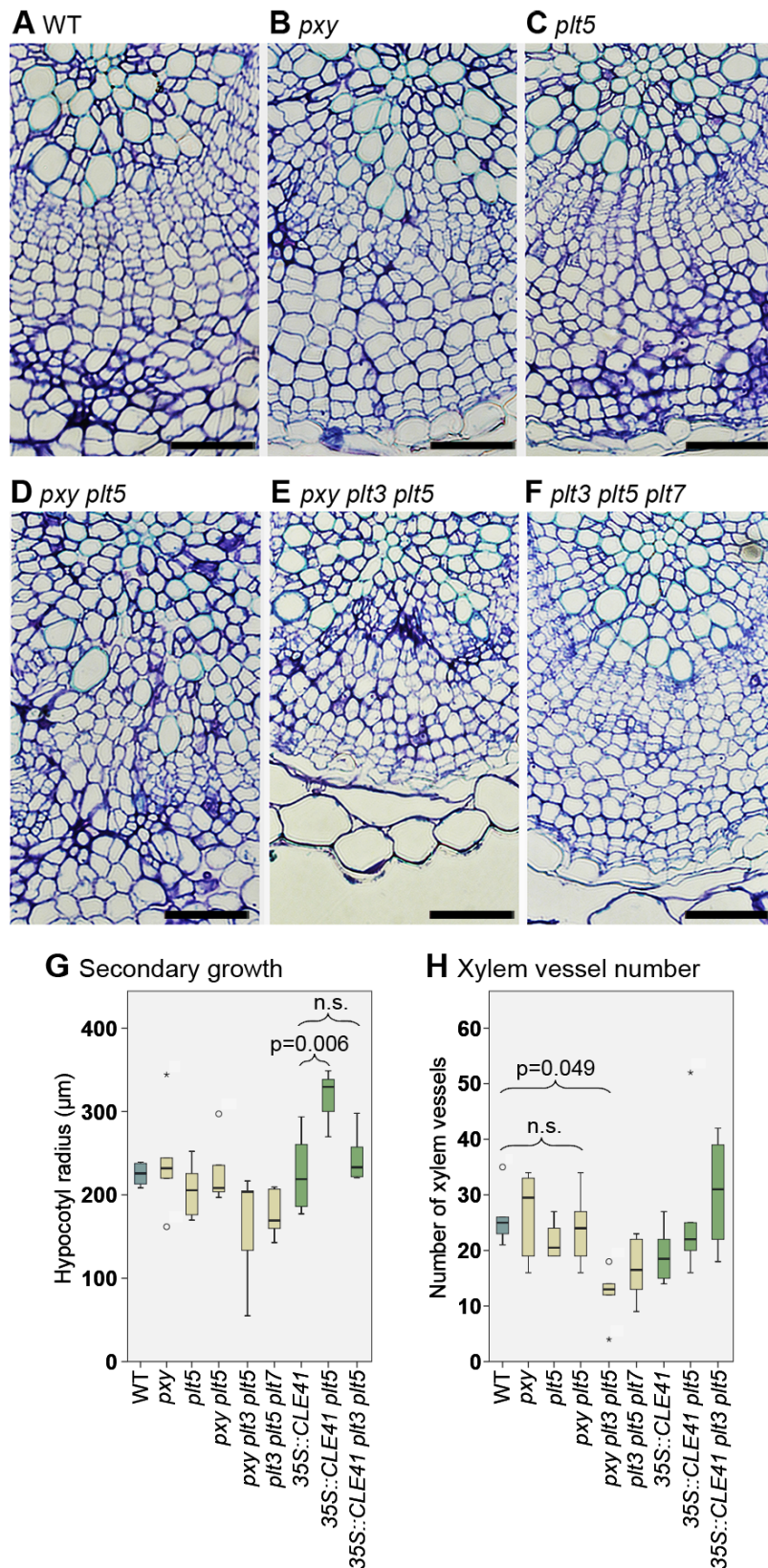


**Figure 13:** Cell radii across genotypes for quantification purposes. (A-F) Show example images utilised for cell radii calculations and a comparison between the genotypes. Shown here is the observable difference between *pxy plt5* double mutant and *pxy plt3 plt5* triple mutant. (G & F) Show graphically the comparison between genotypes for the radii (G) and xylem vessel number (H). This identifies the observational difference between *plt5* mutation in the respective *pxy* and *35S::CLE41* mutation compared to *plt3* and *plt5* in the same backgrounds. This highlights the redundancy and reliance on both genes of *PLT3* and *PLT5*.

## Discussion

Combined analysis suggests that the *PLETHORA* genes act downstream of the PXY element within the signalling and genetic network. A genetic interaction was observed between these two components through morphological analysis of histological stains, yet also highlights the importance of another component in controlling, signalling and interacting with the *PLETHORA* genes within the process of vascular development and the transition to secondary growth process. If the expression of the *PLETHORA* genes that are involved within the secondary growth initiation and development were solely controlled by PXY then one would expect morphological changes of a similar magnitude to those observed in the *pxy* mutants as previously characterised. Further to this, a loss of function mutation would fully attenuate the 35S::CLE41 phenotype. While the observations above identify a novel genetic interaction between PXY and *PLETHORA* genes, another as yet unidentified component may also be involved.

Taken together, the *PLT3* and *PLT5* genes have been identified as being a factor of driving cell proliferation in vascular development, in particular regarding the transition of secondary growth. This is identified and supported by the reduced proliferation in the transgenic line 35S::CLE41 with the *PLETHORA* loss of function mutations (Figure 12). It is supported by previously described RNA-seq data (figure 9). It is possible that changes to distribution of auxin, as has been described in association with *PLETHORA* genes in other developmental processes may also be regulated by these genes.

## **5. GENERATING TOOLS TO FURTHER UNDERSTAND AUXIN AND PIN LOCALISATION BEHAVIOUR REGARDING SECONDARY GROWTH INITIATION.**

### **Background**

The phytohormone auxin is essential for many signalling processes throughout the entire life cycle of the plant. It is responsible for co-ordination and signalling within the plant, and pertinent to this study, the auxin maxima changes during the transition to secondary growth (Reviewed in: Smetana et al., 2019). Whilst several plant hormones, such as cytokinin, have been indicated as partaking within the signalling processes that co-ordinate and regulate vascular tissue formation, considerable evidence exists that indicates auxin as the major signalling element involved in several aspects of the ontogeny (development) of the vascular system (Aloni, 1987; Sachs, 2000), for example, over production of auxin in Arabidopsis transgenic lines leads to increased amount of vascular tissue (Klee et al., 1987).

The PINFORMED1 (PIN1) gene encodes an auxin efflux transmembrane protein responsible for facilitating the transport of auxin between the plasma membrane and intracellular vesicular components (Geldner et al, 2001, Baluska et al, 2003; Paponov et al, 2005). PIN proteins are central to the establishment and maintenance of specific patterns of auxin distribution observed in specific plant tissues (Paponov et al, 2005). Localisation of PIN proteins has been shown to correlate with the direction of auxin movement between cell types often found to be highly polar in many tissues and as such PIN polarity regulates asymmetric auxin distribution. PINs have been shown to be regulated at multiple levels, including endogenous and environmental signals affecting the polarity of localisation (Krecek, 2009). PIN proteins regulate distribution of auxin maxima and are linked to growth and development. An auxin maximum has been well characterised within the root tip and are required for correct specification of cell fates (Sabatini et al, 1999). Auxin maxima persist post embryonically and are required for the maintenance of

the meristem (Sabatini et al, 1999). The PLETHORA (PLT) gene family have been identified as being transcribed in response to auxin accumulation. PLT genes encode transcription factors of the AP2 class (Aida et al, 2004). PLT expression is necessary for root development and maintenance and dependent on the partially redundant transcription factors NPH4 and MP (Leyser, 2005). NPH4 and MP are members of the Q-rich auxin response factor (qARF) family that activates transcription from auxin-inducible genes (Kepinski & Leyser, 2002). At high auxin levels, auxin targets Aux/IAAs for degradation, preventing dimerization between Aux/IAA and qARFs which under low condition levels inhibits transcription (Kepinski & Leyser, 2002).



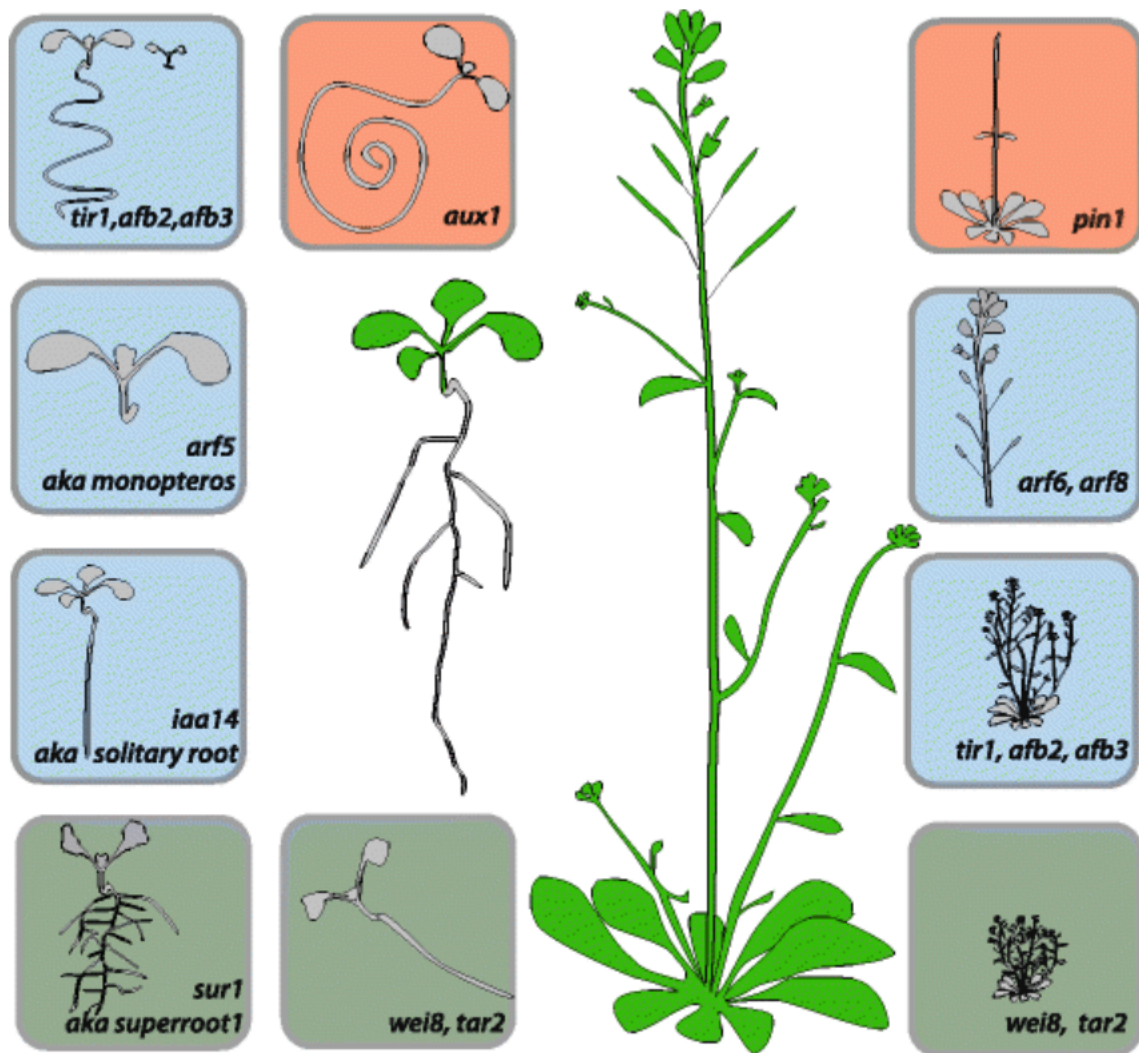


Figure 14: Auxin homeostasis is essential for proper development. Drawings of a wild-type seedling and an adult plant (centre of the figure in green) and some characterized mutants for auxin homeostasis (in boxes). Mutants with affected auxin biosynthesis are in light brown boxes. *sur1* is an overproducer [5] while *wei8 tar2* [6] is depleted of auxin. Signalling mutants are shown in light blue boxes and are mutated in the auxin transcription factor 5 (*arf5/monopteros*) [25], auxin transcriptional inhibitor *iaa14* (or *solitary root*) [26], or the auxin co-receptors (*tir1, afb2, afb3*) [27]. Mutants for influx (*aux1*) [28] and efflux auxin transporters (*pin1*) [7] are shown in the light red boxes (Paque & Weijers., 2016)

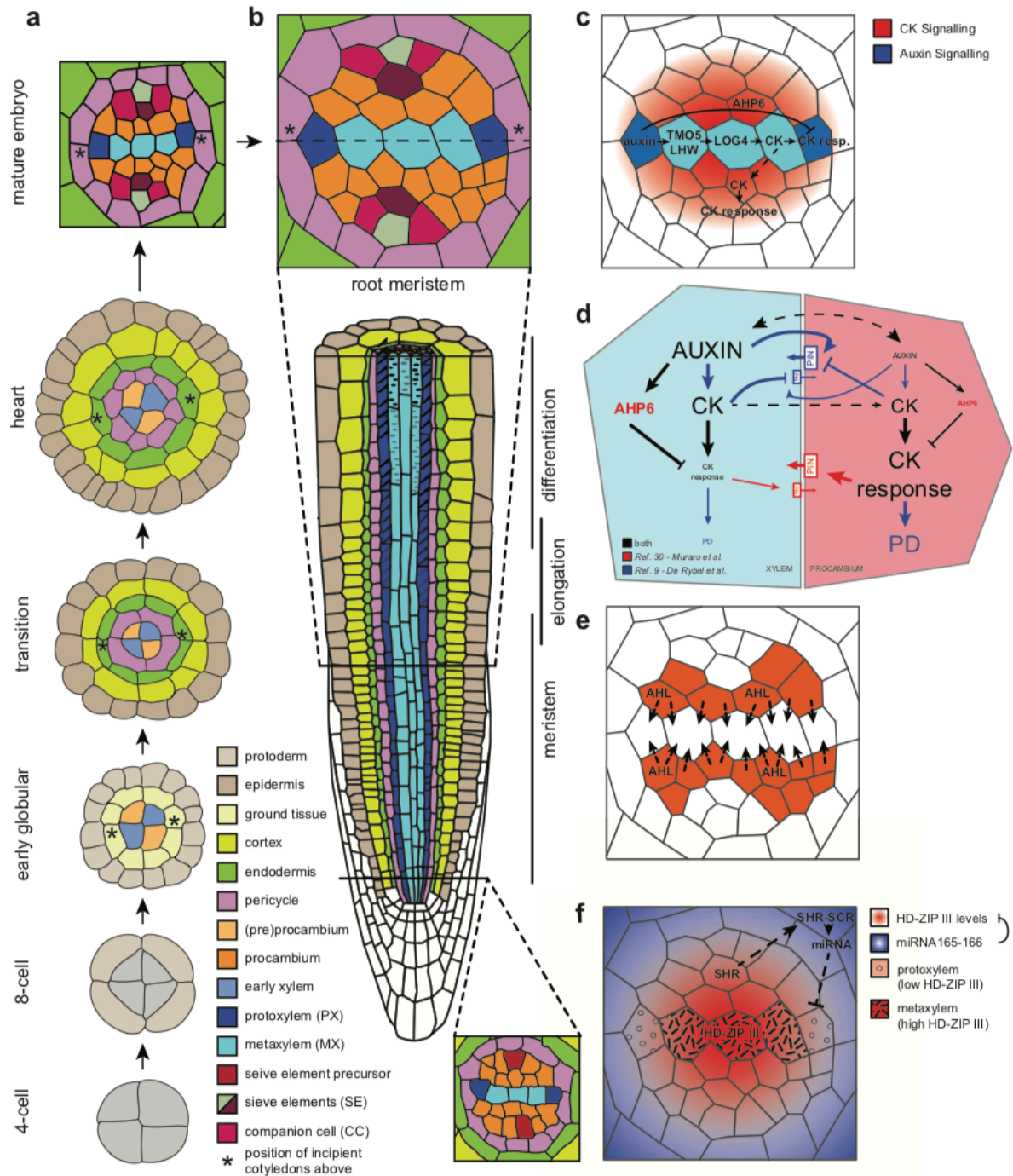


Figure 15: Showing the Aux/IAA interaction at both high and low auxin levels. (A) Ontogeny of the xylem tissues during embryogenesis. Two provascular initial cells share a cellular connection and receive more auxin than the other two through the incipient cotyledons forming above (indicated as asterisk next to early xylem in the e xylem in the early globular stage embryo). These cells will form the xylem axis of the root and are marked by high auxin signalling. The other provascular cells will form procambium and phloem cell lineages, with the procambium marked by high cytokinin (CK) signalling. (B) Schematic longitudinal (lower panel) and radial (upper panel) cross-section through the vascular bundle of the root apical meristem. (C) The Auxin- TMO5/LHW-LOG4-CK pathway controls growth and patterning of the vascular bundle through local production of CK along the xylem axis, which triggers periclinal cell divisions (PD) in the neighbouring procambium cells. (D) Summary of regulatory connections included in computational models describing vascular patterning in the root meristem. (E) The AHL proteins are expressed in procambium cells and migrate towards the xylem axis, thereby controlling strict boundaries between xylem and procambium through an unknown mechanism. (F) Control of metaxylem versus protoxylem identity by the SHR-miR165/166-HD-ZIP III pathway. (De Rybel, Mähönen, Helariutta & Weijers., 2015)

The phytohormone cytokinin also is a regulator of auxin availability (Nieminen et al., 2015). In regard to primary root vasculature development it has been shown that high cytokinin signalling in the procambium promotes an efflux of auxin into the xylem axis through the stimulation of lateralisation of the PINFORMED 1 protein and through increasing the expression of PIN7 and PIN3 (Bishopp et al., 2011). The mutually inhibitory interaction between cytokinin and auxin in adjacent locations maintains the bisymmetric vascular pattern in the primary root (Bishopp et al., 2011).

### Imaging and visualization of vascular morphology through microscopy

One challenge with observing development during secondary growth is the number of cell layers one must penetrate to reach the vascular tissue. There exists a wide range of microscopic methodology and machinery to visualise samples. One such technique is the light sheet fluorescence microscopy (LSFM). The first description of a simplified account of LSFM occurred in 1903 and was termed ultramicroscopy by Siedentopf and Zsigmondy through utilisation of sunlight projection through a slit aperture to observe gold particles. In 1993 orthogonal plane fluorescence optical sectioning (OPFOS) was developed and first described in the literature (Voie et al., 1993). Voie, Burns and Spelman developed the first OPFOS device that could be used for optical sectioning (Voie et al., 1993; Voie & Spelman, 1995; Voie, 1996; Voie 2002). OPFOS featured all of the main essential elements currently present within LSFM devices. These include; laser, beam expander, cylindrical lens for light sheet generation, specimen chamber, orthogonal illumination of the specimen, specimen movement for creation of a z-stack and specimen clearing and staining (Santi, 2011). Nevertheless, it was not until the publication of the selective or single-plane illumination microscopy (SPIM) paper in 2004 (Huisken et al., 2004) that the development and use of LSFM was accelerated due to the article highlighting its ability to investigate embryonic development within the zebrafish. It is now therefore a technique that is growing in popularity within the field of animal development and

room for emergence in plant development. Whilst other LSFMs have been developed since Voie's original description to cater for particular experimental uses, such as Dodt and colleagues adding dual-sided illumination for imaging of larger specimens (Dodt et al., 2007; Becker et al., 2008) the underlying principles of LFSM remain constant across. Light sheet microscopy (LSFM) utilises a thin plane of light that optically sections tissues or even whole organisms (such as the zebrafish embryo). It offers high resolution images and faster imaging speed compared to other non-destructive tomographic devices such as magnetic resonance imaging (MRI) and computerised tomography (CT) (Santi, 2011). LFSM is further distinguished from other microscopic techniques due to its low phototoxicity levels. Light sheet is based upon generation of a sheet of light within the specimen and ensuring that it coincides with focal plane of a high numerical aperture orthogonal objective at 90 degrees. Comparative literature of LFSM against other fluorescent microscopy techniques have previously been published (Fischer et al., 2001; Ripoll et al., 2015; Combs & Shroff, 2007). Particular comparative attention has been drawn against the technology of light sheet fluorescence and confocal fluorescence technologies. One of the major benefits that light sheet pertains over that of confocal microscopy is the specific excitation that reduces the photodamage to the sample and reduces background signals.

A second method of improving imaging deep within large tissues is via clearing methods. Kurihara et al (2015) developed ClearSee as a unique chemical solution to allow deep imaging of morphology and gene expression in plant tissues. They stated that ClearSee rapidly diminishes chlorophyll auto fluorescence while maintaining fluorescent protein stability. By adjusting the refractive index mismatch, whole-organ and whole-plant imaging can be performed by both confocal and two-photo excitation microscopy in ClearSee treated samples (Kurihara et al., 2015). ClearSee is a combination of chemicals xylitol, sodium deoxycholate and urea. Its development sought to address the occurring problem within plant microscopy of

background autofluorescence as plant tissue itself contains and is comprised of a variety of auto fluorescent compounds (Müller et al., 2013). This natural phenomenon presented difficulties for precise microscopic observation of fluorescently tagged proteins in experimental research such as GFP (green fluorescent protein). Further, a variation of refractive indexes within plant tissue components (Kumar & Silva, 1973; Vogelmann et al, 1996) and their mismatch causes light scattering.

### Aims and objectives

Whilst mechanical sectioning is a robust biological tool, it presents problems for reconstruction of a 3D representation of gene expression patterns (Kurihara et al., 2015). Previous chemical reagents such as chloral hydrate (Lersten, 1967) or Hoyer's solution (Hoyer, 1882) had been utilised for clearing and preservation of plant tissue since the late 19<sup>th</sup> century. However, Kurihara sought to develop a clearing dye that could work in correlation and conjunction with fluorescent tagging proteins. ClearSee thus represents an optical clearing reagent for whole-plant fluorescence imaging for enhanced imaging of biological samples.

Experiments described in chapter 4 show that PLT genes lie downstream of PXY signalling element. One hypothesis arising from this is that the genetic interaction between PXY and the *PLETHORA* genes is triggered by auxin maxima changes due to the previously described sensitivity of *PLETHORA* to high auxin levels (Pinon et al., 2012). To investigate these possibilities, we aimed to utilise a GUS reporter system to observe auxin accumulation changes across secondary growth initiation. Such a change would likely be brought about by localisation changes of PIN proteins. Next, we also investigated whether changes in PIN localisation could be detected prior to initiation of secondary growth.

## Results

A DR5::GUS reporter line was crossed with the *pxy* and 35S::CLE41 lines, and *pxy* DR5::GUS, and 35S::CLE41 DR5::GUS lines were identified in the F2 generation due to their DR5::GUS imaging properties. DR5::GUS, *pxy* DR5::GUS, and 35S::CLE41 DR5::GUS plants were grown for 5, 7 and 14 days, stained, fixed, and embedded for sectioning. However, upon sectioning the staining was not visible due to low concentrations of the reporter system in the sections. Qualitative observations made during the staining procedure, suggested that the strength of reporter differed across the time periods investigated. Therefore, further investigation is required, and perhaps by alternative methods for capturing auxin maxima and identifying any changes. Potentially this would lie in alternative fixing procedures. Nevertheless, the genetic resources generated may provide useful tool for future investigation.

Imaging techniques for the visualisation of morphology and gene expression are essential to untangling and biological processes that occur during development. We reasoned that PIN1::GFP tagged lines may be used to enable tracking of changes to auxin homeostasis during secondary growth, visible as PIN1 localisation changes. Visualisation of PIN1 localisation in secondary growth is challenging as changes would be deep within the tissue. In an attempt to address this issue, light-sheet microscopy, combined with the use of Clearsee was investigated. The first question that we addressed was how to best present the sample and orientate it within the machine. The setup of the light-sheet requires the sample to be suspended within a chamber that is positioned perpendicular to the light source. The sample is held within fluid within a chamber, but arranging the tissues proved challenging with 5 day old Arabidopsis seedling root tissue when previously cleared with ClearSee. ClearSee results in optically clear tissue so both retrieving the sample, and keeping it positioned within the chamber aligned for visualisation was problematic. Visualisation of the zebra fish embryo relies on hanging the sample on a hook in the chamber. Consequently, we tried to suspend Arabidopsis roots within optically clear

plastic tubing. Tubing was cut appropriate to size, and to prevent ClearSee liquid leaking in to the fluid chamber of the lightsheet microscope (which contains water); the ends of the clear tubing needed to be tightly sealed. Various materials were tested. Dental gum was found not to dissolve in ClearSee, thus prohibiting potential leaks of clearsee into the microscopy chamber and was thus used in subsequent experiments. In order to attach and insert the sample into the machine it needed to fit on to a loading device. Attachment of the clear tubing to a pipette tip cut in half enabled loading of the sample.

Cut root tissue from the seedlings was loaded in to the tubing device which was filled with fresh ClearSee. The microscope only directs light to a thin and directed area and therefore requires the sample to be positioned appropriately. Locating the root tissue within the tubing was challenging due to a variety of factors. Firstly, cleared root tissue made it very challenging to find. Secondly, as the tubing was larger in size than the sample as it was a liquid filled chamber, the root tissue sample frequently moved and ‘floated’ within the tube. Therefore, even when initially localised, the sample would move during imaging. Lastly, the tubing itself was purchased in a roll, so was curved, presenting a major challenge in terms of alignment of the sample for light sheet scanning and focus. All of these challenges resulted to a particular difficult and time consuming set up. It took multiple attempts and much time trying to locate and identify the sample whilst in the microscopic chamber. Visualisation of z-stacks was performed; however, it did not give the penetration that was required as the inner vascular cylinder was not well defined. Combined with the laborious setup, the decision was then made, in part due to time limitations, to refocus the investigation utilising the confocal microscope. Confocal microscopy is well highly documented within literature for excellent visualisation of tissue. Set up of the sample for this method proved much less challenging. The sample had to be retained in ClearSee liquid, so cover slips were sliced down the middle and located on the



slide either side of the sample, with an intact cover slide placed on top. ClearSee was pipetted in carefully to avoid introduction of air bubbles yet enough to cover the sample. This setup also was essential to prevent the crushing of the root tissue undergoing secondary growth. The confocal microscope works on the principle of point excitation and the point detection of the resulting fluorescence. Images with fluorescence in specific locations were observed. However, upon further examination it became clear that the fluorescence detected was the suberized casparian strip. The confocal could not provide sufficient illumination of the vascular cylinder. The casparian strip also prevented access of counter-stains to cells in the vascular cylinder. Thus, it was not possible to accurately determine the localisation of PIN proteins.

## Discussion

The experiments above describe some method development. With further research it may be possible to track the PIN localisation changes with the tagging of PIN proteins. One possibility would be to section tissue with a vibratome and visualise transverse sections under the confocal, as used by Smetana et al. (2019). Alternatively, methods for immobilising whole roots stained with ClearSee, e.g. by adding an optically clear gelling agent may enable use of light sheet microscopy.

As the literature describes the auxin maxima localisation changes during secondary growth, it is likely that this would be coupled with changes in localisation of PIN efflux carriers. PLT1, PLT2 and PLT3 have been shown to redundantly control expression of multiple *PIN* genes in the embryonic and post-embryonic root (Galinha et al., 2007). I speculate that the interaction between PLT, PINs and auxin may also be involved in a feedback loop during secondary growth, that is somehow influenced by PXY signalling. Here, we were unable to test this hypothesis.



## 6. INVESTIGATING INTERACTIONS BETWEEN TMO6 & WOX14 TRANSCRIPTION FACTORS

### Background

Mapping of putative PXY-mediated transcriptional regulatory network using yeast-1-hybrid described by Smit et al, 2020, has identified many more putative PXY-regulated mechanisms. Among these, transcription factors TARGET OF MONOPTEROS6 (TMO6) and WUSCHEL HOMEODOMAIN RELATED14 (WOX14) were identified as regulating the expression of a gene that encodes a third transcription factor; LATERAL ORGAN BOUNDARIES DOMAIN4 (LBD4). PXY signalling and auxin were found to regulate the WOX14, TMO6, LBD4 feedforward loop which, in turn, controlled vascular proliferation (Smit et al., 2020; Figure 16). This is shown in the figure through cell count number significantly reduced comparative to a WT cell count within the vascular bundle for the mutated lines in the LBD4, WOX14 and TMO6 transgenic lines. This observation is depicted visually through qualitative microscopy images of the specific lines that displays the morphological changes as a consequence of mutations in the genes.

PXY signalling results in the upregulation of WOX14 transcription factor genes (Hirakawa et al., 2010; Etchells et al., 2013). MONOPTEROS (MP), an auxin response factor (Hardtke & Berleth, 1998) controls expression of TMO6 (Schlereth et al., 2010). TMO6 encodes the DOF family of transcription factors that are known for promotion of vascular cell divisions (Guo et al., 2009; Waki et al., 2013; Konishi et al., 2015; Miyashima et al., 2019; Smet et al., 2019). The genetic interactions observed between LBD4 and PXY suggested that the role of LBD4 is to marking the phloem-procambium boundaries and thus define the edges of the vascular meristem (Smit et al., 2020).

A prerequisite for *in planta* transcriptional regulation within the feed-forward loop is expression of TMO6, WOX14 and LBD4 in the same place and time. TMO6 and LBD4 mRNA was present in the inflorescence stem vascular tissue with expression maxima at the phloem-procambium boundary. WOX14::GUS expression was also present in phloem-procambium boundary cells, in addition to other vascular cell types (Etchells et al., 2013).

Given the genetic interaction and overlapping expression, evidence for the feed-forward loop interactions identified in yeast-1-hybrid were sought *in planta*. Work done by Heng utilised *Nicotiana* leaf protoplasts for transformation with a construct that harboured LBD4pro::LUC (LUCIFERASE). LUC activity in cells co-transformed with both LBD4pro::LUC reporter and a 35S::TMO6 construct, was higher than that observed in cells transformed with the LBD4pro::LUC reporter with a control (Figure 17). LBD4 promoter activity was further increased when cells were co-transformed with both LBD4pro::LUC, 35S::TMO6, and 35S::WOX14 plasmids (Heng, unpublished). One explanation for this observation is that there may be a physical interaction between WOX14 and TMO6.

The yeast II hybrid system technique allows the detection of interacting proteins in living yeast cells (Fields & Song, 1989). Two fusion, also termed hybrids, are constructed between each protein, or in this case transcription factor, of interest. The hybrids constructed are comprised of either the DNA binding domain (DBD) or the activation domain (AD). The protein or transcription factor of interest in the experiment is referred to the ‘bait’ and the ‘prey’ for the DNA binding domain and activation domain respectively. Connection of the two elements (transcription factor and DBD/AD) within the vector genome results in attachment of the transcribed proteins. If the two proteins (transcription factors) of interest, the ‘bait’ and the ‘prey’, directly interact with one another it brings the DBD and AD within close enough

proximity for functionality of the transcription factor for the promoter and synthesis of the biosynthesis gene.

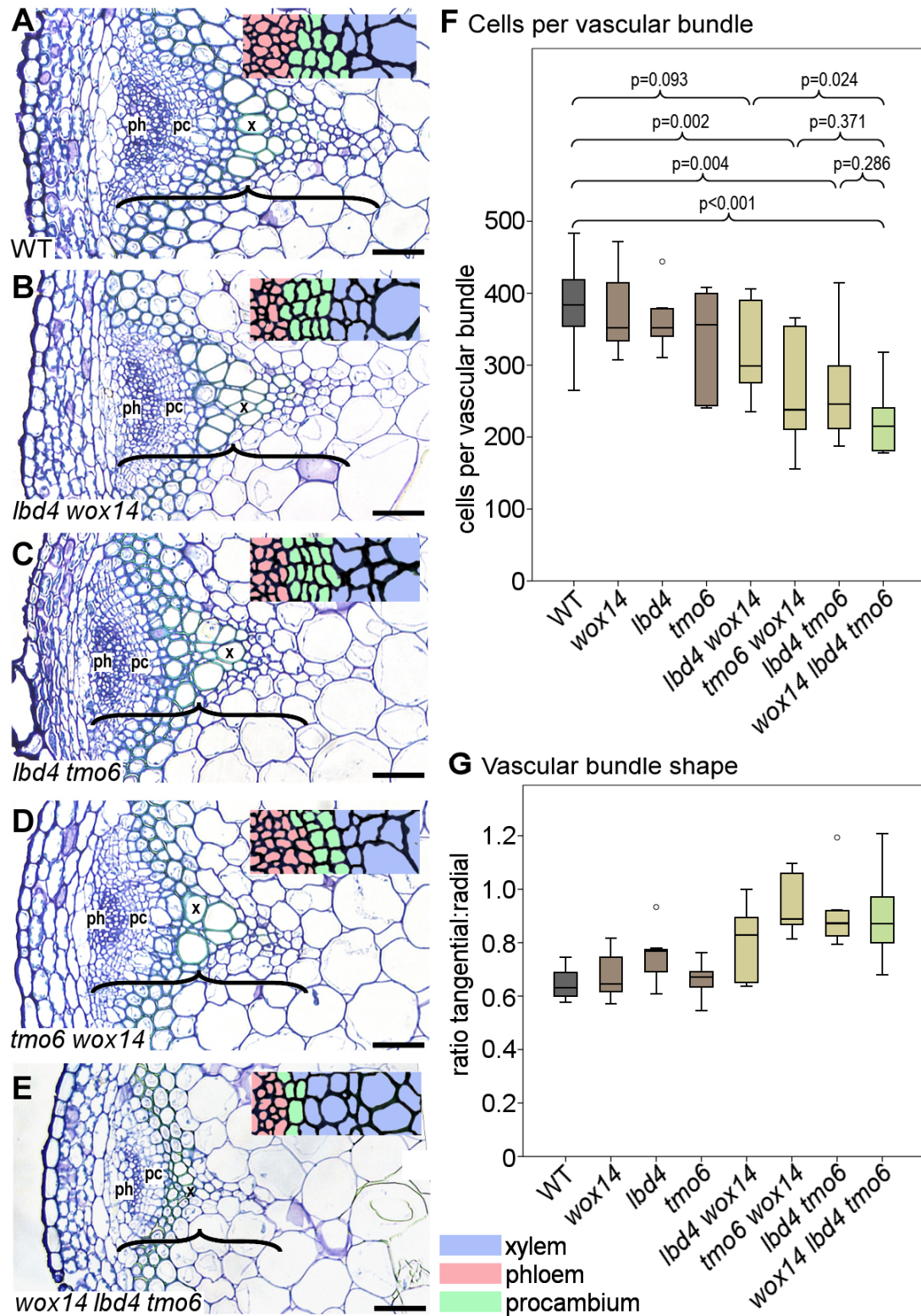
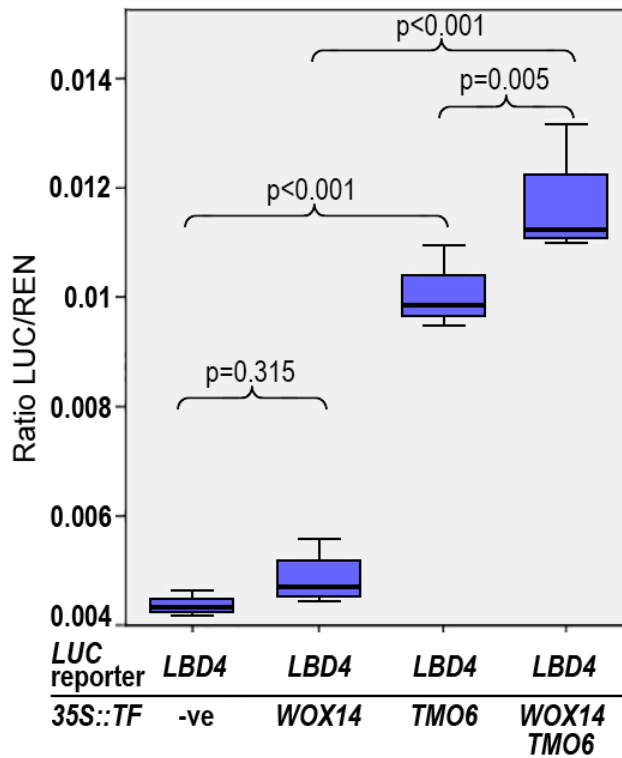


**Figure 16:** “Consequences of Removing the Feed-Forward Loop.(A) to (E) Morphology of vascular bundles from inflorescence stems in the wild type (A), *lbd4 wox14* (B), *lbd4 tmo6* (C), *tmo6 wox14* (D), and *wox14 lbd4 tmo6* (E). Transverse sections were stained with toluidine blue. Insets show closeups of the cambium (green). pc, cambium; ph, phloem; x, xylem. Brackets mark the vascular bundle size along the radial axis of the stem. Bars = 50 μm.(F) Boxplots showing mean number of cells per vascular bundle in *wox14 lbd4 tmo6* and double and single mutant controls. Significant differences were determined by ANOVA with an LSD posthoc test ( $n = 6$ ). (G) Boxplot showing vascular bundle shape determined by measuring the ratio of tangential to radial axis ( $n = 6$ ). Boxplots show median (inner line) and inner quartiles (box). Whiskers extend to the highest and lowest values no greater than 1.5 times the inner quartile range, and circles show outliers.” (Smit et al., 2020)

**A** WOX14 and TMO6 activate expression from the *LBD4* promoter



**B** WOX14 activates the *TMO6* promoter

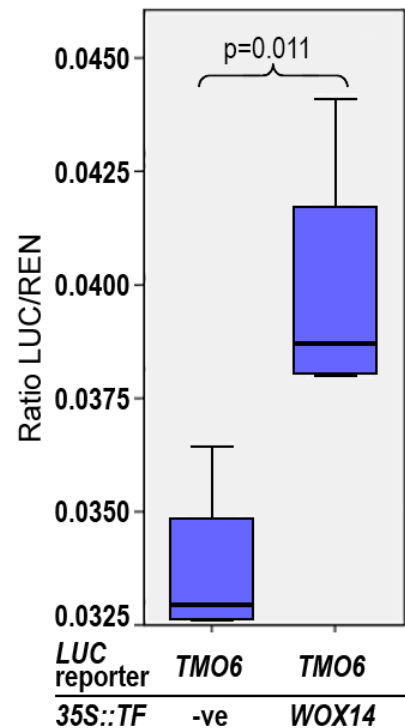


**Figure 17:** Graphical results: *Nicotiana leaf protoplasts* were transformed with a construct that harboured *LBD4pro::LUC* (*LUCIFERASE*). *LUC* activity in cells co-transformed with both *LBD4pro::LUC* reporter and a *35S::TMO6* construct, was higher than that observed in cells transformed with the *LBD4pro::LUC* reporter with a control. *LBD4* promoter activity was further increased when cells were co-transformed with both *LBD4pro::LUC*, *35S::TMO6*, and *35S::WOX14* plasmids (Provided in full by Heng, Unpublished)

### Aims and objectives

Due to the work done by Heng, it was hypothesised that the TMO6 and WOX14 transcription factors may directly interact. To test this experimentally a yeast II hybrid approach was undertaken. Direct interaction of the TMO6 transcription factor with that of WOX14 would be supported through activation of biosynthesis genes.

### Results

A yeast II hybrid approach was undertaken. Direct interaction of the TMO6 transcription factor with that of WOX14 would be supported through activation of biosynthesis genes for production of leucine and tryptophan (Figure 18). For the purposes of this experiment the vectors PGAD T7, containing ampicillin resistance and the leucine biosynthesis gene, and vector PGBK T7, containing the kanamycin resistance and tryptophan biosynthesis gene, were utilised. Upon analysis sequence data, and NdeI restriction site was identified in the WOX14 cDNA sequence allowed use for cloning into WOX14 pGAD T7 and pGBK T7. WOX14 primers were generated utilising the primer 3 online primer design tool. Reverse primers were modified to include the sequences for the restriction enzymes Pst1 and Xho1 for subsequent ligation into vectors (Primers shown in table 2 in chapter 2). Previously acquired complementary DNA (cDNA) from WT Arabidopsis was acquired from laboratory stocks as template for PCR amplification of WOX14 coding sequence.

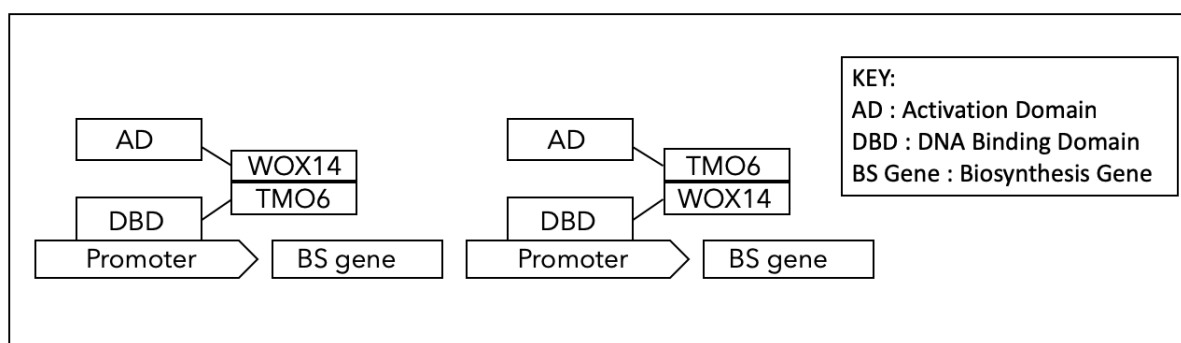


**Figure 18:** Theoretical diagram for yeast two hybrid system testing set up. Wox14 and TMO6 ORF sizes are 65 and 55 respectively.

For PCR amplification of TMO6, the primer 3 online analysis tool could not identify any desirable primers. The first 29 base pairs of TMO6 were taken with an addition of ‘CAT’ to the 5’ end added to allow the inclusion of an Nde1 site necessary for the restriction digest and ligation of PCR products into the vectors in the later experimental stage. Hairpin formation in these primers was analysed utilising an online biotools (Northwestern University, Chicago). A BLAST analysis confirmed that the primer sequence were unique. Reverse primers were designed similarly, but with Pst1 and Xho1 restriction site sequences included. Primers for TMO6 are shown in table 3 in Chapter 2. WOX14 and TMO6 cDNA’s were cloned into pJET 1.2 where they were sequenced, and were subsequently cloned into pGAD T7 and pGBK T7.

## Discussion

Due to time limitations only 3 out of the intended 4 combination pairings were obtained. These were obtained and stored in glycerol stocks for future experimental work. In future work the yeast II hybrid system could be used to test if TMO6 and WOX14 physically interact.

## 7. GENERAL DISCUSSION

To conclude, the research described as part of this thesis have shown that there exists a genetic interaction between the PXY gene and those of the *PLETHORA3* and *PLETHORA5* genes in *Arabidopsis thaliana*. This thesis has shown that *PLETHORA3* and *PLETHORA5* genes act redundantly and are in part responsible for the process of cell proliferation during secondary growth. The loss of function mutations in *PLT3* and *PLT5* result in enhanced phenotypes in *pxy* background, and the suppression of hallmark characteristics, loss of vascular organisation and cell proliferation in transgenic 35S::CLE41 overexpression backgrounds. PXY is a central factor within the vascular development network and has been shown, not only this work, but in the literature, to be an important factor of vascular development (Etchells., 2013; Etchells & Turner., 2010; Fischer & Turner., 2010; Figure 5; Figure 9; Figure 13). Previously PXY was known to be important in the regulation of cellular organisation and proliferation throughout the process of secondary growth; now, however, this work has shown the importance of a genetic interaction of PXY with the *PLETHORA* family of genes in regard to cellular control of proliferation. However, it is also clear that it is just one element of a complex signalling network. It is clear that other interacting factors are also extremely important for the development of the vasculature. Addressed within this thesis is the role that *ERECTA-LIKE* and *PLETHORA* genes play with regards to interactions with PXY. It has been shown that the *ERECTA-LIKE* genes interact with PXY to regulate the cell size in vascular cell types, and I have shown that *PLETHORA* interacts to drive proliferation within the vascular cambium in regards to secondary growth. This work has also set the foundation for further research in relation to the possible physical interaction of the two transcription factors TMO6 and WOX14, which could be tested in future using the yeast II hybrid system.

The limitations of this study in regard to the quantitative analysis lies in the low *n* used to gauge *PXY-PLT* genetic interactions. This is due to limited time and the future study in this area



should verify the findings here via experimentation on a larger scale. Looking forward with this work it would be of interest to determine if a genetic interaction exists between the *PLETHORA* and *ERECTA* family members themselves. Determination of an interaction between these families could point to *PLT* acting downstream of *PXY* and ER signalling. This would be facilitated through generation of *ERf* lines in a *plt3 plt5 plt7* knockout background, alongside investigation with the *ERL1* and *ERL2* lines with both singular, double and triple *PLETHORA* knockouts. Further, studies should also look to determine and reveal the spatial expression of *PLETHORA* and identify potential targets.

In addition, for completeness of the study, it would be important to utilise a qRT-PCR across the genotypes that have been generated. Analysis of expression data could identify downstream targets, potentially *WOX4* or *WOX14* that are already known as downstream targets of *pxy*, and further support the claims made here.

### Implications of this research

Aside from the importance of uncovering the molecular mechanisms and genetic interactions, the wider implications of this research are represented in the application of this knowledge within tree species and utilisation for manipulation for increased production for the biomass industry. Many of the genes that have been found to be up-regulated within wood-forming stems have auxin responsive cis-acting elements within their promoter region (Jae-Heung Ko, Park & Yang, 2004). It has already been shown by Etchells et al that wood formation in trees is increased by manipulating *PXY*-regulated cell division with ectopic overexpression of *PttPXY* and *PttCLE41*, cloned putative orthologs genes in hybrid aspen. This resulted in vascular tissue abnormalities and poor plant growth, yet precise tissue-specific overexpression generated trees that exhibited a 2-fold increase in the rate of wood formation, were taller, and possessed larger leaves compared to their controls. (Etchells., 2015b) The advancement of

knowledge within the field of vascular development, in particular advances in knowledge attained through this study, identifies promise for the future in a world of uncertainty with an ever increasing need to switch to more renewable resources.

## 8. REFERENCES

- Abrash, E. B., Davies, K. A., and Bergmann, D. C., 2011.** Generation of Signaling Specificity in Arabidopsis by Spatially Restricted Buffering of Ligand–Receptor Interactions. *The Plant Cell*, 23 (8), 2864–2879.
- Agusti, J., Herold, S., Schwarz, M., Sanchez, P., Ljung, K., Dun, E. A., Brewer, P. B., Beveridge, C. A., Sieberer, T., Sehr, E. M., and Greb, T., 2011.** Strigolactone signaling is required for auxin-dependent stimulation of secondary growth in plants. *Proceedings of the National Academy of Sciences*, 108 (50), 20242–20247.
- Aida, M., Beis, D., Heidstra, R., Willemsen, V., Blilou, I., Galinha, C., Nussaume, L., Noh, Y.-S., Amasino, R., and Scheres, B., 2004.** The PLETHORA Genes Mediate Patterning of the Arabidopsis Root Stem Cell Niche. *Cell*, 119 (1), 109–120.
- Aloni, R., 1987. Differentiation of Vascular Tissues. *Annual Review of Plant Physiology*, 38 (1), 179–204.
- Bagdassarian, K. S., Connor, K. A., Jermyn, I. H., and Etchells, J., 2019.** Versatile method for quantifying and analyzing morphological differences in experimentally obtained images. *Plant Signaling & Behavior*, 15 (1), 1693092.
- Baluska, F., 2003.** Polar transport of auxin: carrier-mediated flux across the plasma membrane or neurotransmitter-like secretion? *Trends in Cell Biology*, 13 (6), 282–285.
- Baucher, M., Jaziri, M. E., and Vandeputte, O., 2007.** From primary to secondary growth: origin and development of the vascular system. *Journal of Experimental Botany*, 58 (13), 3485–3501.
- Baum, S. F., Dubrovsky, J. G., and Rost, T. L., 2002.** Apical organization and maturation of the cortex and vascular cylinder in *Arabidopsis thaliana* (Brassicaceae) roots. *American Journal of Botany*, 89 (6), 908–920.
- Becker, K., Jährling, N., Kramer, E. R., Schnorrer, F., and Dodt, H.-U., 2008.** Ultramicroscopy: 3D reconstruction of large microscopical specimens. *Journal of Biophotonics*, 1 (1), 36–42.
- Beeckman, T. and Smet, I. D., 2014.** Pericycle. *Current Biology*, 24 (10).
- Bell, C. J. and Maher, E. P., 1990.** Mutants of *Arabidopsis thaliana* with abnormal gravitropic responses. *Molecular and General Genetics MGG*, 220 (2), 289–293.

- Benková, E., Michniewicz, M., Sauer, M., Teichmann, T., Seifertová, D., Jürgens, G., and Friml Jiří, 2003.** Local, Efflux-Dependent Auxin Gradients as a Common Module for Plant Organ Formation. *Cell*, 115 (5), 591–602.
- Bennett, M. J., Marchant, A., Green, H. G., May, S. T., Ward, S. P., Millner, P. A., Walker, A. R., Schulz, B., and Feldmann, K. A., 1996.** Arabidopsis AUX1 Gene: A Permease-Like Regulator of Root Gravitropism. *Science*, 273 (5277), 948–950.
- Berg, C. V. D., Willemsen, V., Hendriks, G., Weisbeek, P., and Scheres, B., 1997.** Short-range control of cell differentiation in the Arabidopsis root meristem. *Nature*, 390 (6657), 287–289.
- Bhalerao, R. P. and Fischer, U., 2014.** Auxin gradients across wood - instructive or incidental? *Physiologia Plantarum*, 151 (1), 43–51.
- Bishopp, A., Help, H., El-Showk, S., Weijers, D., Scheres, B., Friml, J., Benková, E., Mähönen, A. and Helariutta, Y., 2011.** A Mutually Inhibitory Interaction between Auxin and Cytokinin Specifies Vascular Pattern in Roots. *Current Biology*, 21(11), pp.917-926.
- Busse, J. S. and Evert, R. F., 1999.** Vascular Differentiation and Transition in the Seedling of Arabidopsis thaliana (Brassicaceae). *International Journal of Plant Sciences*, 160 (2), 241–251.
- Chaffey, N., Cholewa, E., Regan, S., and Sundberg, B., 2002.** Secondary xylem development in Arabidopsis: a model for wood formation. *Physiologia Plantarum*, 114 (4), 594–600.
- Combs, C. A. and Shroff, H., 2017.** Fluorescence Microscopy: A Concise Guide to Current Imaging Methods. *Current Protocols in Neuroscience*, 79 (1).
- De Rybel, B., Möller, B., Yoshida, S., Grabowicz, I., Barbier De Reuille, P., Boeren, S., Smith, R. S., Borst, J. W., and Weijers, D., 2013.** A bHLH Complex Controls Embryonic Vascular Tissue Establishment and Indeterminate Growth in Arabidopsis. *Developmental Cell*, 24 (4), 426–437.
- De Rybel, B., Mähönen, A., Helariutta, Y. and Weijers, D., 2015.** Plant vascular development: from early specification to differentiation. *Nature Reviews Molecular Cell Biology*, 17(1), pp.30-40.

**Dhonukshe, P., Huang, F., Galvan-Ampudia, C. S., Mahonen, A. P., Kleine-Vehn, J., Xu, J., Quint, A., Prasad, K., Friml, J., Scheres, B., and Offringa, R., 2010.** Plasma membrane-bound AGC3 kinases phosphorylate PIN auxin carriers at TPRXS(N/S) motifs to direct apical PIN recycling. *Development*, 137 (19), 3245–3255.

**Dodt, H.-U., Leischner, U., Schierloh, A., Jährling, N., Mauch, C. P., Deininger, K., Deussing, J. M., Eder, M., Zieglgänsberger, W., and Becker, K., 2007.** Ultramicroscopy: three-dimensional visualization of neuronal networks in the whole mouse brain. *Nature Methods*, 4 (4), 331–336.

**Dolan L., Janmaat K., Willemsen V., Linstead P., Poethig S., Roberts K., Scheres B. 1993.** Cellular organisation of the Arabidopsis thaliana root. *Development*.;119(1):71–84

**Etchells, J. P. and Turner, S. R., 2010.** The PXY-CLE41 receptor ligand pair defines a multifunctional pathway that controls the rate and orientation of vascular cell division. *Development*, 137 (5), 767–774.

**Etchells, J. P., Provost, C. M., Mishra, L., and Turner, S. R., 2013.** WOX4 and WOX14 act downstream of the PXY receptor kinase to regulate plant vascular proliferation independently of any role in vascular organisation. *Development*, 140 (10), 2224–2234.

**Etchells, J. P., Smit, M. E., Gaudinier, A., Williams, C. J., and Brady, S. M., 2015.** A brief history of the TDIF-PXY signalling module: balancing meristem identity and differentiation during vascular development. *New Phytologist*, 209 (2), 474–484.

**Etchells, J., Mishra, L., Kumar, M., Campbell, L. and Turner, S., 2015b.** Wood Formation in Trees Is Increased by Manipulating PXY-Regulated Cell Division. *Current Biology*, 25(8), pp.1050-1055.

**Fields, S. and Song, O.-K., 1989.** A novel genetic system to detect protein–protein interactions. *Nature*, 340 (6230), 245–246.

**Fischer, R. S., Wu, Y., Kanchanawong, P., Shroff, H., and Waterman, C. M., 2011.** Microscopy in 3D: a biologists toolbox. *Trends in Cell Biology*, 21 (12), 682–691.

**Fisher, K. and Turner, S., 2007.** PXY, a Receptor-like Kinase Essential for Maintaining Polarity during Plant Vascular-Tissue Development. *Current Biology*, 17 (12), 1061–1066.

**Friml, J., Vieten, A., Sauer, M., Weijers, D., Schwarz, H., Hamann, T., Offringa, R., and Jürgens, G., 2003.** Efflux-dependent auxin gradients establish the apical–basal axis of Arabidopsis. *Nature*, 426 (6963), 147–153.

**Fàbregas, N., Formosa-Jordan, P., Confraria, A., Siligato, R., Alonso, J. M., Swarup, R., Bennett, M. J., Mähönen, A. P., Caño-Delgado, A. I., and Ibañez, M., 2015.** Auxin Influx Carriers Control Vascular Patterning and Xylem Differentiation in Arabidopsis thaliana. *PLOS Genetics*, 11 (4).

**Galinha, C., Hofhuis, H., Luijten, M., Willemsen, V., Blilou, I., Heidstra, R., and Scheres, B., 2007.** PLETHORA proteins as dose-dependent master regulators of Arabidopsis root development. *Nature*, 449 (7165), 1053–1057.

**Ga Lweiler, L., Guan, C., Mu Ller, A., Wisman, E., Mendgen, K., Yephremov, A., and Palme, K., 1998.** Regulation of Polar Auxin Transport by AtPIN1 in Arabidopsis Vascular Tissue. *Science*, 282 (5397), 2226–2230.

**Geldner, N., Friml, J., Stierhof, Y.-D., Jürgens, G., and Palme, K., 2001.** Auxin transport inhibitors block PIN1 cycling and vesicle trafficking. *Nature*, 413 (6854), 425–428.

**Goldsmith, M. H. M., 1977.** The Polar Transport of Auxin. *Annual Review of Plant Physiology*, 28 (1), 439–478.

**Guo, Y., Qin, G., Gu, H., and Qu, L.-J., 2009.** Dof5.6/HCA2, a Dof Transcription Factor Gene, Regulates Interfascicular Cambium Formation and Vascular Tissue Development in Arabidopsis. *The Plant Cell*, 21 (11), 3518–3534.

**Hardtke, C. S. and Berleth, T., 1998.** The Arabidopsis gene MONOPTEROS encodes a transcription factor mediating embryo axis formation and vascular development. *The EMBO Journal*, 17 (5), 1405–1411.

**Hay, A. and Tsiantis, M., 2006.** The genetic basis for differences in leaf form between Arabidopsis thaliana and its wild relative Cardamine hirsuta. *Nature Genetics*, 38 (8), 942–947.

**Heisler, M. G., Ohno, C., Das, P., Sieber, P., Reddy, G. V., Long, J. A., and Meyerowitz, E. M., 2005.** Patterns of Auxin Transport and Gene Expression during Primordium Development Revealed by Live Imaging of the Arabidopsis Inflorescence Meristem. *Current Biology*, 15 (21), 1899–1911.

**Hemerly, A. S., Ferreira, P. C., Montagu, M. V., and Inzé, D., 1999.** Cell cycle control and plant morphogenesis: is there an essential link? *BioEssays*, 21 (1), 29–37.

**Hirakawa, Y., Shinohara, H., Kondo, Y., Inoue, A., Nakanomyo, I., Ogawa, M., Sawa, S., Ohashi-Ito, K., Matsubayashi, Y., and Fukuda, H., 2008.** Non-cell-autonomous control of vascular stem cell fate by a CLE peptide/receptor system. *Proceedings of the National Academy of Sciences*, 105 (39), 15208–15213.

**Hirakawa, Y., Kondo, Y., and Fukuda, H., 2010.** TDIF Peptide Signaling Regulates Vascular Stem Cell Proliferation via the WOX4 Homeobox Gene in Arabidopsis. *The Plant Cell*, 22 (8), 2618–2629.

**Horvitz, H. R. and Sternberg, P. W., 1991.** Multiple intercellular signalling systems control the development of the *Caenorhabditis elegans* vulva. *Nature*, 351 (6327), 535–541.

**Hoyer, H., 1882.** Beiträge zur anatomischen und histologischen Technik. *Archiv für Mikroskopische Anatomie*, 13 (1), 645–650.

**Huisken, J., 2004.** Optical Sectioning Deep Inside Live Embryos by Selective Plane Illumination Microscopy. *Science*, 305 (5686), 1007–1009.

**Ikematsu, S., Tasaka, M., Torii, K. U., and Uchida, N., 2017.** ERECTA-family receptor kinase genes redundantly prevent premature progression of secondary growth in the Arabidopsis hypocotyl. *New Phytologist*, 213 (4), 1697–1709.

**Ingham, P. W., 1988.** The molecular genetics of embryonic pattern formation in *Drosophila*. *Nature*, 335 (6192), 744–744.

**Ito, Y., Nakanomyo, I., Motose, H., Iwamoto, K., Sawa, S., Dohmae, N., and Fukuda, H., 2006.** Dodeca-CLE Peptides as Suppressors of Plant Stem Cell Differentiation. *Science*, 313 (5788), 842–845.

**Jonsson, H., Heisler, M. G., Shapiro, B. E., Meyerowitz, E. M., and Mjolsness, E., 2006.** An auxin-driven polarized transport model for phyllotaxis. *Proceedings of the National Academy of Sciences*, 103 (5), 1633–1638.

**Kimura, T., Haga, K., Shimizu-Mitao, Y., Takebayashi, Y., Kasahara, H., Hayashi, K.-I., Kakimoto, T., and Sakai, T., 2018.** Asymmetric Auxin Distribution is Not Required to Establish Root Phototropism in Arabidopsis. *Plant and Cell Physiology*, 59 (4), 828–840.

**Kepinski, S., and Leyser, O. 2002.** Ubiquitination and auxin signaling: A degrading story. *Plant Cell* 14 (suppl.), S81.–S95.

- Klee, H. J., Horsch, R. B., Hinchee, M. A., Hein, M. B., and Hoffmann, N. L., 1987.** The effects of overproduction of two *Agrobacterium tumefaciens* T-DNA auxin biosynthetic gene products in transgenic petunia plants. *Genes & Development*, 1 (1), 86–96.
- Ko, J.-H., Han, K.-H., Park, S., and Yang, J., 2004.** Plant Body Weight-Induced Secondary Growth in *Arabidopsis* and Its Transcription Phenotype Revealed by Whole-Transcriptome Profiling. *Plant Physiology*, 135 (2), 1069–1083.
- Ko, J.-H., Han, K.-H., Park, S., and Yang, J., 2004.** Plant Body Weight-Induced Secondary Growth in *Arabidopsis* and Its Transcription Phenotype Revealed by Whole-Transcriptome Profiling. *Plant Physiology*, 135 (2), 1069–1083.
- Konishi, M., Donner, T. J., Scarpella, E., and Yanagisawa, S., 2015.** MONOPTEROS directly activates the auxin-inducible promoter of the Dof5.8 transcription factor gene in *Arabidopsis thaliana* leaf provascular cells. *Journal of Experimental Botany*, 66 (1), 283–291.
- Kumar, R. and Silva, L., 1973.** Light Ray Tracing Through a Leaf Cross Section. *Applied Optics*, 12 (12), 2950.
- Kurihara, D., Mizuta, Y., Sato, Y., and Higashiyama, T., 2015.** ClearSee: a rapid optical clearing reagent for whole-plant fluorescence imaging. *Development*, 142 (23), 4168–4179.
- Křeček, P., Skůpa, P., Libus, J., Naramoto, S., Tejos, R., Friml, J., and Zažímalová, E., 2009.** The PIN-FORMED (PIN) protein family of auxin transporters. *Genome Biology*, 10 (12), 249.
- Leyser, O., 2005.** Auxin Distribution and Plant Pattern Formation: How Many Angels Can Dance on the Point of PIN? *Cell*, 121 (6), 819–822.
- Lucas, W. J., Groover, A., Lichtenberger, R., Furuta, K., Yadav, S.-R., Helariutta, Y., He, X.-Q., Fukuda, H., Kang, J., Brady, S. M., Patrick, J. W., Sperry, J., Yoshida, A., López-Millán, A.-F., Grusak, M. A., and Kachroo, P., 2013.** The Plant Vascular System: Evolution, Development and FunctionsF. *Journal of Integrative Plant Biology*, 55 (4), 294–388.
- Mahonen, A. P., 2000.** A novel two-component hybrid molecule regulates vascular morphogenesis of the *Arabidopsis* root. *Genes & Development*, 14 (23), 2938–2943.



- Mahonen, A. P., 2006.** Cytokinin Signaling and Its Inhibitor AHP6 Regulate Cell Fate During Vascular Development. *Science*, 311 (5757), 94–98.
- Mayer, U., Ruiz, R. A. T., Berleth, T., Miséra, S., and Jürgens, G., 1991.** Mutations affecting body organization in the Arabidopsis embryo. *Nature*, 353 (6343), 402–407.
- Meyerowitz, E. M., 1989.** Arabidopsis, a useful weed. *Cell*, 56 (2), 263–269.
- Miyashima, S., Koi, S., Hashimoto, T., and Nakajima, K., 2011.** Non-cell-autonomous microRNA165 acts in a dose-dependent manner to regulate multiple differentiation status in the Arabidopsis root. *Development*, 138 (11), 2303–2313.
- Miyashima, S., Roszak, P., Sevilem, I., Toyokura, K., Blob, B., Heo, J.-O., Mellor, N., Help-Rinta-Rahko, H., Otero, S., Smet, W., Boekschoten, M., Hooiveld, G., Hashimoto, K., Smetana, O., Siligato, R., Wallner, E.-S., Mähönen, A. P., Kondo, Y., Melnyk, C. W., Greb, T., Nakajima, K., Sozzani, R., Bishopp, A., Rybel, B. D., and Helariutta, Y., 2019.** Mobile PEAR transcription factors integrate positional cues to prime cambial growth. *Nature*, 565 (7740), 490–494.
- Mähönen, A. P., Tusscher, K. T., Siligato, R., Smetana, O., Díaz-Triviño, S., Salojärvi, J., Wachsman, G., Prasad, K., Heidstra, R., and Scheres, B., 2014.** PLETHORA gradient formation mechanism separates auxin responses. *Nature*, 515 (7525), 125–129.
- Müller, S. M., Galliardt, H., Schneider, J., Barisas, B. G., and Seidel, T., 2013.** Quantification of Förster resonance energy transfer by monitoring sensitized emission in living plant cells. *Frontiers in Plant Science*, 4.
- Nieminen, K., Blomster, T., Helariutta, Y., and Mähönen, A. P., 2015.** Vascular Cambium Development. *The Arabidopsis Book*, 13.
- Nüsslein-Vollhard, C. 1991.** Determination of the embryonic axes of Drosophila. Development Supplement 1, 1-10.
- Ohashi-Ito, K. and Bergmann, D. C., 2007.** Regulation of the Arabidopsis root vascular initial population by LONESOME HIGHWAY. *Development*, 134 (16), 2959–2968.

- Ohashi-Ito, K., Matsukawa, M., and Fukuda, H., 2013.** An Atypical bHLH Transcription Factor Regulates Early Xylem Development Downstream of Auxin. *Plant and Cell Physiology*, 54 (3), 398–405.
- Okada, K. and Shimura, Y., 1990.** Reversible Root Tip Rotation in Arabidopsis Seedlings Induced by Obstacle-Touching Stimulus. *Science*, 250 (4978), 274–276.
- Okada, K., Ueda, J., Komaki, M. K., Bell, C. J., and Shimura, Y., 1991.** Requirement of the Auxin Polar Transport System in Early Stages of Arabidopsis Floral Bud Formation. *The Plant Cell*, 3 (7), 677.
- Paponov, I., Teale, W., Trebar, M., Blilou, I., and Palme, K., 2005.** The PIN auxin efflux facilitators: evolutionary and functional perspectives. *Trends in Plant Science*, 10 (4), 170–177.
- Paque, S. and Weijers, D., 2016.** Q&A: Auxin: the plant molecule that influences almost anything. *BMC Biology*, 14(1).
- Petrasek, J. and Friml, J., 2009.** Auxin transport routes in plant development. *Development*, 136 (16), 2675–2688.
- Pinon, V., Prasad, K., Grigg, S. P., Sanchez-Perez, G. F., and Scheres, B., 2012.** Local auxin biosynthesis regulation by PLETHORA transcription factors controls phyllotaxis in Arabidopsis. *Proceedings of the National Academy of Sciences*, 110 (3), 1107–1112.
- Prasad, K., Grigg, S. P., Barkoulas, M., Yadav, R. K., Sanchez-Perez, G. F., Pinon, V., Blilou, I., Hofhuis, H., Dhonukshe, P., Galinha, C., Mähönen, A. P., Muller, W. H., Raman, S., Verkleij, A. J., Snel, B., Reddy, G. V., Tsiantis, M., and Scheres, B., 2011.** Arabidopsis PLETHORA Transcription Factors Control Phyllotaxis. *Current Biology*, 21 (13), 1123–1128.
- Ragni, L., Nieminen, K., Pacheco-Villalobos, D., Sibout, R., Schwechheimer, C., and Hardtke, C. S., 2011.** Mobile Gibberellin Directly Stimulates Arabidopsis Hypocotyl Xylem Expansion. *The Plant Cell*, 23 (4), 1322–1336.
- Reinhardt, D., Mandel, T., and Kuhlemeier, C., 2000.** Auxin Regulates the Initiation and Radial Position of Plant Lateral Organs. *The Plant Cell*, 12 (4), 507.

**Reinhardt, D., Pesce, E.-R., Stieger, P., Mandel, T., Baltensperger, K., Bennett, M., Traas, J., Friml, J., and Kuhlemeier, C., 2003.** Regulation of phyllotaxis by polar auxin transport. *Nature*, 426 (6964), 255–260.

**Reuille, P. B. D., Bohn-Courseau, I., Ljung, K., Morin, H., Carraro, N., Godin, C., and Traas, J., 2006.** Computer simulations reveal properties of the cell-cell signaling network at the shoot apex in Arabidopsis. *Proceedings of the National Academy of Sciences*, 103 (5), 1627–1632.

**Ripoll, J., Koberstein-Schwarz, B., and Ntziachristos, V., 2015.** Unleashing Optics and Optoacoustics for Developmental Biology. *Trends in Biotechnology*, 33 (11), 679–691.

**Roman, G., Lubarsky, B., Kieber, J. J., Rothenberg, M. and Ecker, J. R. 1995.** Genetic-analysis of ethylene signal transduction in Arabidopsis thaliana: five novel mutant loci integrated into a stress-response pathway. *Genetics* 139,1393 -1409.

**Rybel, B. D., Mähönen, A. P., Helariutta, Y., and Weijers, D., 2015.** Plant vascular development: from early specification to differentiation. *Nature Reviews Molecular Cell Biology*, 17 (1), 30–40.

**Sabatini, S., Beis, D., Wolkenfelt, H., Murfett, J., Guilfoyle, T., Malamy, J., Benfey, P., Leyser, O., Bechtold, N., Weisbeek, P., and Scheres, B., 1999.** An Auxin-Dependent Distal Organizer of Pattern and Polarity in the Arabidopsis Root. *Cell*, 99 (5), 463–472.

**Sachs, T., 2000.** Integrating Cellular and Organismic Aspects of Vascular Differentiation. *Plant and Cell Physiology*, 41 (6), 649–656.

**Santi, P. A., 2011.** Light Sheet Fluorescence Microscopy. *Journal of Histochemistry & Cytochemistry*, 59 (2), 129–138.

**Santuari, L., Sanchez-Perez, G. F., Luijten, M., Rutjens, B., Terpstra, I., Berke, L., Gorte, M., Prasad, K., Bao, D., Timmermans-Hereijgers, J. L., Maeo, K., Nakamura, K., Shimotohno, A., Pencik, A., Novak, O., Ljung, K., Heesch, S. V., Bruijn, E. D., Cuppen, E., Willemsen, V., Mähönen, A. P., Lukowitz, W., Snel, B., Ridder, D. D., Scheres, B., and Heidstra, R., 2016.** The PLETHORA Gene Regulatory Network Guides Growth and Cell Differentiation in Arabidopsis Roots. *The Plant Cell*, 28 (12), 2937–2951.

**Scheres B., Wolkenfelt H., Willemsen V., . Terlouw M, Lawson E., Dean C., . Weisbeek P., 1994** Embryonic origin of the Arabidopsis primary root and root meristem initials *Development* 120: 2475-2487;

**Schlereth, A., Möller, B., Liu, W., Kientz, M., Flipse, J., Rademacher, E. H., Schmid, M., Jürgens, G., and Weijers, D., 2010.** MONOPTEROS controls embryonic root initiation by regulating a mobile transcription factor. *Nature*, 464 (7290), 913–916.

**Shobe, W. R. and Lersten, N. R., 1967.** A Technique for Clearing and Staining Gymnosperm Leaves. *Botanical Gazette*, 128 (2), 150–152.

**Shpak, E. D., 2004.** Synergistic interaction of three ERECTA-family receptor-like kinases controls Arabidopsis organ growth and flower development by promoting cell proliferation. *Development*, 131 (7), 1491–1501.

**Shpak, E. D., Lakeman, M. B., and Torii, K. U., 2003.** Dominant-Negative Receptor Uncovers Redundancy in the Arabidopsis ERECTA Leucine-Rich Repeat Receptor–Like Kinase Signaling Pathway That Regulates Organ Shape. *The Plant Cell*, 15 (5), 1095–1110.

**Sibout, R., Plantegenet, S., and Hardtke, C. S., 2008.** Flowering as a Condition for Xylem Expansion in Arabidopsis Hypocotyl and Root. *Current Biology*, 18 (6), 458–463.

**Smet, W., Seville, I., Balaguer, M. A. D. L., Wybouw, B., Mor, E., Miyashima, S., Blob, B., Roszak, P., Jacobs, T. B., Boekschoten, M., Hooiveld, G., Sozzani, R., Helariutta, Y., and Rybel, B. D., 2019.** DOF2.1 Controls Cytokinin-Dependent Vascular Cell Proliferation Downstream of TMO5/LHW. *Current Biology*, 29 (3).

**Smetana, O., Mäkilä, R., Lyu, M., Amiryousefi, A., Rodríguez, F. S., Wu, M.-F., Solé-Gil, A., Gavarrón, M. L., Siligato, R., Miyashima, S., Roszak, P., Blomster, T., Reed, J. W., Broholm, S., and Mähönen, A. P., 2019.** High levels of auxin signalling define the stem-cell organizer of the vascular cambium. *Nature*, 565 (7740), 485–489.

**Smit, M. E., McGregor, S. R., Sun, H., Gough, C., Bågman, A.-M., Soyars, C. L., Kroon, J. T., Gaudinier, A., Williams, C. J., Yang, X., Nimchuk, Z. L., Weijers, D., Turner, S. R., Brady, S. M., and Etchells, J. P., 2019.** A PXY-Mediated Transcriptional Network Integrates Signaling Mechanisms to Control Vascular Development in Arabidopsis. *The Plant Cell*, 32 (2), 319–335.

Somerville, C., 2006. Cellulose Synthesis in Higher Plants. *Annual Review of Cell and Developmental Biology*, 22 (1), 53–78.

**Swarup, K., Benková, E., Swarup, R., Casimiro, I., Péret, B., Yang, Y., Parry, G., Nielsen, E., Smet, I. D., Vanneste, S., Levesque, M. P., Carrier, D., James, N., Calvo, V., Ljung, K., Kramer, E., Roberts, R., Graham, N., Marillonnet, S., Patel, K., Jones, J. D., Taylor, C. G., Schachtman, D. P., May, S., Sandberg, G., Benfey, P., Friml, J., Kerr, I., Beeckman, T., Laplace, L., and Bennett, M. J., 2008.** The auxin influx carrier LAX3 promotes lateral root emergence. *Nature Cell Biology*, 10 (8), 946–954.

**Torii, K. U., Mitsukawa, N., Oosumi, T., Matsuura, Y., Yokoyama, R., Whittier, R. F., and Komeda, Y., 1996.** The Arabidopsis ERECTA gene encodes a putative receptor protein kinase with extracellular leucine-rich repeats. *The Plant Cell*, 8 (4), 735–746.

**Uchida, N., Lee, J. S., Horst, R. J., Lai, H.-H., Kajita, R., Kakimoto, T., Tasaka, M., and Torii, K. U., 2012.** Regulation of inflorescence architecture by intertissue layer ligand-receptor communication between endodermis and phloem. *Proceedings of the National Academy of Sciences*, 109 (16), 6337–6342.

**Uchida, N. and Tasaka, M., 2013.** Regulation of plant vascular stem cells by endodermis-derived EPFL-family peptide hormones and phloem-expressed ERECTA-family receptor kinases. *Journal of Experimental Botany*, 64 (17), 5335–5343.

**Uchida, N., Shimada, M., and Tasaka, M., 2013.** ERECTA-Family Receptor Kinases Regulate Stem Cell Homeostasis via Buffering its Cytokinin Responsiveness in the Shoot Apical Meristem. *Plant and Cell Physiology*, 54 (3), 343–351.

**Ullah, H., 2001.** Modulation of Cell Proliferation by Heterotrimeric G Protein in Arabidopsis. *Science*, 292 (5524), 2066–2069.

**Veylder, L. D., Beeckman, T., Beemster, G. T., Engler, J. D. A., Ormenese, S., Maes, S., Naudts, M., Schueren, E. V. D., Jacquemard, A., Engler, G., and Inzé, D., 2002.** Control of proliferation, endoreduplication and differentiation by the Arabidopsis E2Fa-DPa transcription factor. *The EMBO Journal*, 21 (6), 1360–1368.

- Vogelmann, T. C., Bornman, J. F., and Yates, D. J., 1996.** Focusing of light by leaf epidermal cells. *Physiologia Plantarum*, 98 (1), 43–56.
- Voie, A. H., Burns, D. H., and Spelman, F. A., 1993.** Orthogonal-plane fluorescence optical sectioning: Three-dimensional imaging of macroscopic biological specimens. *Journal of Microscopy*, 170 (3), 229–236.
- Voie, A. H. and Spelman, F. A., 1995.** Three-dimensional reconstruction of the cochlea from two-dimensional images of optical sections. *Computerized Medical Imaging and Graphics*, 19 (5), 377–384.
- Voie AH. 1996.** Three-dimensional reconstruction and quantitative analysis of the mammalian cochlea [dissertation]. [Seattle (WA)]: University of Washington
- Voie, A. H., 2002.** Imaging the intact guinea pig tympanic bulla by orthogonal-plane fluorescence optical sectioning microscopy. *Hearing Research*, 171 (1-2), 119–128.
- Wachsman, G., Sparks, E. E., and Benfey, P. N., 2015.** Genes and networks regulating root anatomy and architecture. *New Phytologist*, 208 (1), 26–38.
- Waki, T., Miyashima, S., Nakanishi, M., Ikeda, Y., Hashimoto, T., and Nakajima, K., 2013.** A GAL4-based targeted activation tagging system in *Arabidopsis thaliana*. *The Plant Journal*, 73 (3), 357–367.
- Wang, N., Bagdassarian, K. S., Doherty, R. E., Kroon, J. T., Connor, K. A., Wang, X. Y., Wang, W., Jermyn, I. H., Turner, S. R., and Etchells, J. P., 2019.** Organ-specific genetic interactions between paralogues of the PXY and ER receptor kinases enforce radial patterning in *Arabidopsis* vascular tissue. *Development*, 146 (10).
- Whitford, R., Fernandez, A., Groodt, R. D., Ortega, E., and Hilson, P., 2008.** Plant CLE peptides from two distinct functional classes synergistically induce division of vascular cells. *Proceedings of the National Academy of Sciences*, 105 (47), 18625–18630.
- Wisniewska, J., Xu, J., Seifertová, D., Brewer, P. B., Ruzicka, K., Blilou, I., Rouquié, D., Benková, E., Scheres, B., and Friml, J., 2006.** Polar PIN Localization Directs Auxin Flow in Plants. *Science*, 312 (5775), 883–883.
- Zhou, X. and Su, Z., 2007.** EasyGO: Gene Ontology-based annotation and functional enrichment analysis tool for agronomical species. *BMC Genomics*, 8 (1), 246.